

Accounts

Superconductivity of Ternary Metal Compounds Prepared at High Pressures

Ichimin Shirotani

Faculty of Engineering, Muroran Institute of Technology, 27-1, Mizumoto, Muroran-shi 050-8585

(Received February 14, 2002)

Various ternary metal phosphides, arsenides, antimonides, silicides and germanides have been prepared at high temperatures and high pressures. These ternary metal compounds can be classified into four groups: [1] metal-rich compounds MM'_4X_2 and [2] MM′X, [3] non-metal-rich compounds MXX′ and [4] MM'_4X_{12} (M and M′ = metal element; X and X′ = non-metal element). We have studied the electrical and magnetic properties of these materials at low temperatures, and found many new superconductors with the superconducting transition temperature (T_c) of above 10 K. The metal-rich compound $ZrRu_4P_2$ with a tetragonal structure showed the superconducting transition at around 11 K, and had an upper critical field (H_{c2}) of 12.2 tesla (T) at 0 K. Ternary equiatomic compounds ZrRuP and ZrRuSi crystallize in two modifications, a hexagonal Fe_2P-type structure [h-ZrRuP(Si)] and an orthorhombic Co_2P-type structure [o-ZrRuP(Si)]. Both h-ZrRuP and h-ZrRuSi have rather high T_c values of above 12 K; on the contrary, T_c of o-ZrRuP and o-ZrRuSi is about 4 K. The alloys $ZrRu_{1-x}Rh_xP$ were prepared at high temperatures and at high pressures. The superconductivity and the crystal structure of the alloys are very sensitive to the content of Rh atoms. The H_{c2} values of h-ZrRuP, h-HfRuP, h-ZrRuSi and h-ZrRuAs are 14–16 T at 0 K. The coherence length of these compounds is below 50 Å. ZrRhSi with the Co_2P-type structure and ZrRuGe with a TiFeSi-type structure showed the superconductivity at around 10.5 K. T_c's of MoNiP with the Fe_2P-type structure and MoRuP with the Co_2P-type structure were over 15 K. Both compounds have the highest T_c among the metal phosphides. Non-metal-rich compound NbPS showed the T_c of 13 K and the high H_{c2} of 17 T. This H_{c2} value is the highest among the phosphide superconductors. The Debye temperature and the density of states at the Fermi level for NbPS are 330 K and 0.51 states/eV-atom, respectively. Filled skutterudites $LnRu_4X_{12}$ (Ln = La and Pr, X = P, As and Sb) with a cubic structure show interesting superconductivity behavior at low temperatures. $LaRu_4As_{12}$ had the highest T_c of 10.3 K among the skutterudite compounds. $PrRu_4As_{12}$ with the magnetic element Pr transformed to a superconductor at around 2.4 K. Superconducting properties of various ternary metal compounds prepared at high pressure are discussed.

Ternary metal compounds are constructed by three elements with a non-metal atom. These elements occupy a distinct set of crystallographic lattice sites. Only part of the valence electrons of the metal are involved in bonding with the non-metal element and the excess valence electrons partially fill the conduction band formed by the overlap of s-, p- and d-orbitals of the elements. Generally, ternary metal compounds exhibit high electrical conductivity and metallic behavior. Since a large number of ternary metal compounds have been discovered, these compounds do seem to offer a better scope for the realization of high superconducting transition temperatures (T_c) and high critical magnetic fields (H_{c2}).[1] However, the electrical and magnetic properties of ternary metal compounds have not been studied sufficiently yet.

A number of ternary metal compounds such as phosphide and silicide show the characteristic structure with clusters consisting of metal and non-metal atoms in the crystal. The superconducting ternary metal compounds mainly can be classified into four main groups: metal-rich compounds [1] MM'_4X_2 and [2] MM′X, non-metal rich compounds [3] MXX′ and [4] MM'_4X_{12} (M and M′ = metal elements; X and X′ = non-metal elements). The ratio of metal and non-metal elements and the crystal structures of these materials are summarized in Table 1. Cluster structures constructed by metal or non-metal atoms exist in the crystal. We have prepared ternary metal phosphides, arsenides, antimonides, silicides and germanides at high temperatures and high pressures. Several ternary metal

Table 1. Ratio of Metal and Non-metal Elements and Crystal Structure of Ternary Metal Compounds Prepared at High Pressure

Compounds	Metal:Non-metal	Structure	Peculiarity of structure
MM'_4X_2	5:2	$ZrFe_4Si_2$-type	tetrahedral M_4 clusters
MM′X	2:1	Fe_2P-type	
		Co_2P-type	trianglar M_3 clusters
		TiFeSi-type	
MXX′	1:2	NbPS-type	M_2 and X_2 clusters
MM'_4X_{12}	5:12	$LaFe_4P_{12}$-type	square X_4^{4-} clusters

Published on the web July 15, 2003; DOI 10.1246/bcsj.76.1291

compounds exhibit the superconductivity with rather high T_c of above 10 K.[2] Vandenberg and Matthias have suggested a few guidelines for the prediction of superconductivity in binary and ternary metal compounds.[3] The T_c of a material is found to be a sensitive function of the crystal symmetry, atom clustering, lattice instabilities and number of valence electrons. Clustering of metal or non-metal atoms is an important feature of the high T_c superconductors.

Metal-rich compounds ZrM_4P_2 (M = transition metal) crystallize with a tetragonal $ZrFe_4Si_2$-type structure, space group $P4_2/mnm$.[4] These phosphides have the characteristic structure with tetrahedral M_4 clusters in a marcasite-type host structure. The M_4 clusters with common edges develop as infinite linear chains along the [100] direction. New compounds $ZrRu_4P_2$ and $HfRu_4P_2$ have been prepared at around 850 °C and 4 GPa; the superconducting transition of both compounds is observed at around 10 K.[5]

Ternary equiatomic compounds with the general formula MM′X are known, where M is a large, electropositive transition metal from the left side of the periodic table, while M′ is a small transition metal, and X is P, As, Si or Ge. For the equiatomic compounds the ordered versions of Fe_2P-, Co_2P (TiNiSi)- and TiFeSi-type with layer structures most frequently occur.[6] Equiatomic compounds show the interesting electrical and magnetic properties at low temperatures. With the presence of the 3d transition metals Cr, Mn, Fe, Co or Ni, most of the compounds reported are ordered ferromagnetically.[7]

ZrRuP crystallizes in two modifications: a hexagonal Fe_2P-type structure (h-ZrRuP)[8] and an orthorhombic Co_2P-type structure (o-ZrRuP).[9] h-ZrRuP has the two-dimensional triangular clusters of Ru atoms. The orthorhombic phase of ZrRuP transforms to the hexagonal Fe_2P-type structure at around 1100 °C and 3.5 GPa.[10] Many MM′X compounds that include 4d transition metal behave as the superconductors with rather high T_c of above 10 K.[8,11–13]

NbPS is a non-metal rich equiatomic compound. The crystal structure of NbPS is orthorhombic with the space group *Immm*.[14] There are interesting structural features with Nb–Nb and P–P dimers in continuous strings. The compound transforms to a superconductor at around 12 K.[14,15] Keszler and Hoffmann have performed tight binding band structure calculations for NbPS.[16]

Non-metal rich compounds with the general formula LnM_4X_{12} (Ln = lanthanide; M = Fe, Ru and Os; X = pnicogen) crystallize in a skutterudite ($CoAs_3$-type) structure filled by lanthanide atoms.[17–19] This structure is cubic, space group $Im\bar{3}$, $Z = 2$. Ln atoms locate at (000) and (1/2 1/2 1/2) of a cubic structure like bcc. The transition metal atoms (T) are in the center of a distorted octahedral environment of six pnicogen atoms. The skutterudite-type structure is characterized by the formation of well-defined X_4^{4-} groups. These filled skutterudites show the anomalous electrical and magnetic behavior at low temperatures.[20,21] One of the most striking features of these compounds is the occurrence of the superconductivity for $LaFe_4P_{12}$ with T_c of 4.1 K.[22] We have found two interesting new superconductor: $LaRu_4As_{12}$ and $PrRu_4As_{12}$.[23] $LaRu_4As_{12}$ has the highest T_c of 10.3 K among the skutterudite compounds. $PrRu_4As_{12}$ is an superconductor ($T_c = 2.4$ K) with a magnetic element Pr. On the other hand, $PrRu_4P_{12}$ shows the metal to insulator transition at around 60 K.[24] The heavy-fermion superconductor $PrOs_4Sb_{12}$ was recently found at around 1.85 K.[25,26]

We have prepared many ternary metal compounds at high temperatures and at high pressures and found many new superconductors with a T_c value of above 10 K. In this report, the interesting superconductivity of various ternary metal compounds prepared at high pressure is discussed.

High-Pressure Synthesis. Using a wedge-type cubic-anvil high pressure apparatus, ternary metal compounds were prepared at high temperatures and high pressures.[11] The upper and lower stages of the high pressure apparatus consist of three anvils that slide on the wedge formed in shallow V-shaved grooves. The anvil movement is completely synchronized by means of a wedge system. The anvils prepared from cemented tungsten carbide have a 16×16 mm^2 top-square face. The sample container made of pyrophyllite is formed into a cube of 21 mm on an edge. Figure 1 shows the sample assembly for the preparation of the ternary metal compounds. This system is similar to that used for the high-pressure synthesis of black phosphorus.[27,28] Starting materials are put into a crucible made of BN. The crucible with a graphite heater is then inserted into the pyrophyllite cube.

We prepared various ternary metal phosphides, arsenides, antimonides, silicides and germanides at high temperatures and high pressures. The ternary metal compounds were prepared by reaction of stoichiometric amounts of each metal and non-metal powder at around 4 GPa. The reaction temperatures were between 800 and 1600 °C. Samples were characterized by powder X-ray diffraction using Cu Kα radiation and silicon as a standard.

Copper or gold lead wire was attached to polycrystals of the

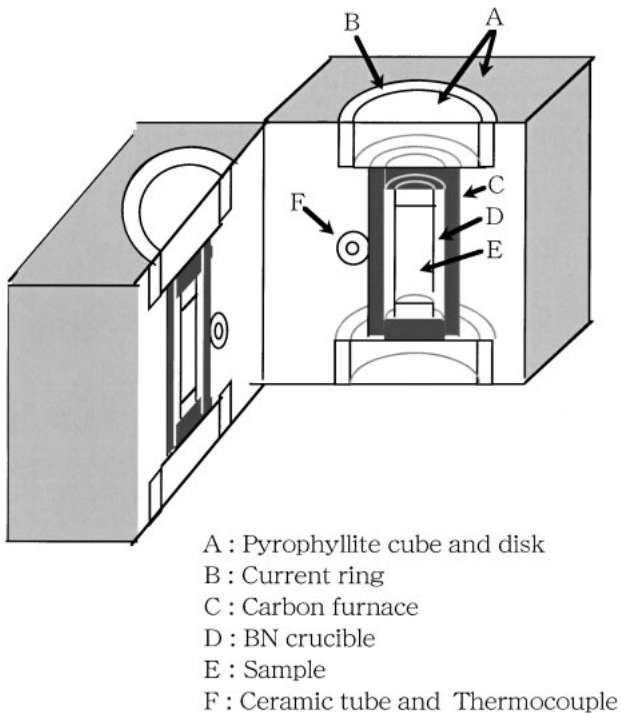

Fig. 1. Sample assembly for the high-pressure synthesis of ternary metal compounds.

samples with silver filled by epoxy, and four-lead electrical resistivity measurements were performed at low temperatures. The resistances of the samples were measured as a function at applied magnetic field at constant low temperatures. The dc magnetic susceptibility of the polycrystalline samples was measured in the range of 1.8–300 K with a Quantum Design SQUID magnetometer. Specific-heat measurements for the samples were performed in the temperature range between 2 and 20 K.

Results and Discussion

We have prepared various ternary metal compounds with T_c of above 10 K at high temperatures and high pressures. The superconducting materials are classified into four groups: metal-rich compounds [1] MM'_4X_2 and [2] $MM'X$; non-metal-rich compounds [3] MXX' and [4] MM'_4X_{12} (M and M′ = metal elements; X and X′ = non-metal elements). The crystal data of the main superconducting materials are summarized in Table 2.

[1] Metal-Rich Compounds MRu_4P_2 (M = Zr and Hf). Ternary metal phosphides ZrM_4P_2 (M = Fe and Ni) crystallize with a tetragonal $ZrFe_4Si_2$-type structure, space group $P4_2/mnm$.[4] Figure 2 shows the crystal structure of $ZrNi_4P_2$. The compounds have the characteristic structure with tetrahedral M_4 clusters in a marcasite-type host structure. The M_4 clusters with common edges develop as infinite linear chains along the [001] direction. The magnetic properties of $ZrNi_4P_2$ show the temperature-independent susceptibility, which indicates the Pauli paramagnetism of the conduction electrons. Extended Hückel molecular orbital and tight binding band structure calculations have been carried out for $ZrNi_4P_2$.[29]

Figure 3 shows the resistivity vs temperature curves of $ZrRu_4P_2$ prepared at around 850 °C and 4 GPa. The structure of this compound is similar to that of $ZrNi_4P_2$.[4] The crystal data of $ZrRu_4P_2$ are $a = 6.992(3)$ Å, $c = 3.699(3)$ Å, $V = 180.8(2)$ Å^3 and $Z = 2$. The resistivity rapidly decreases with decreasing temperature, and sharply drops at around 11 K.[5] Figure 4 shows the temperature dependence of dc magnetic susceptibility measured in an applied field of 5 *Oe* for the polycrystalline sample of $ZrRu_4P_2$. The existence of hysteresis between zero-field cooling (ZFC) and field cooling (FC) indicates that the phosphide is a type Ⅱ superconductor. When the reaction temperature is over 950 °C, the resistivity does not become zero at around the superconducting transition

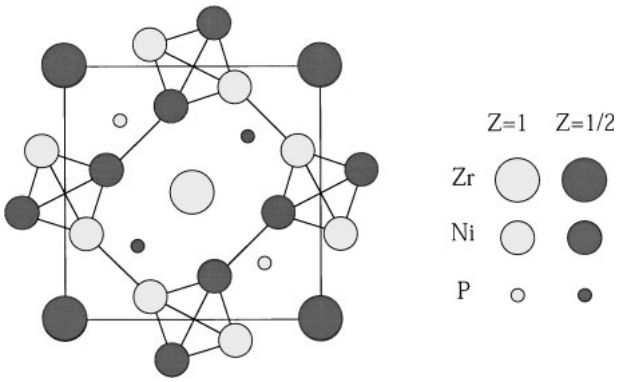

Fig. 2. Crystal structure of $ZrNi_4P_2$.

temperature.[30] This tendency becomes more remarkable for the higher reaction temperatures. The electrical properties of $HfRu_4P_2$ are similar to those of $ZrRu_4P_2$. The superconducting transition of the Hf compound is observed at around 9.5 K.[30] $ZrNi_4P_2$ does not show any superconductivity down to 2 K.

The resistance of $ZrRu_4P_2$ is measured as a function of the applied magnetic field at constant temperatures between 0.6 and 8.4 K. The T_c decreases with increasing applied magnetic field. The superconducting transition becomes broader at lower temperatures. Figure 5 shows the upper critical field (H_{c2}) vs temperature curve for $ZrRu_4P_2$. The H_{c2}–T curve shown by a dotted line is fitted by the pair breaking model.[39] The H_{c2}

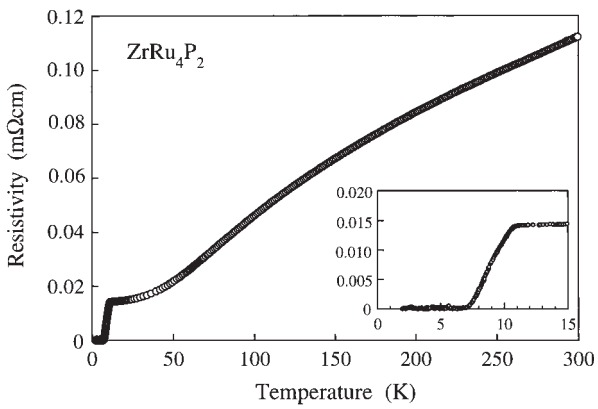

Fig. 3. Resistivity vs temperature curve of $ZrRu_4P_2$ prepared at around 850 °C and 4 GPa.

Table 2. Crystal Data of Ternary Metal Compounds

	Structure		Lattice constants/Å			volume/one atom
			a	*b*	*c*	Å^3
$ZrRu_4P_2$	tetragonal	$ZrNi_4P_2$-type	6.992	—	3.699	12.9
h-ZrRuP	hexagonal	Fe_2P-type	6.459	—	3.778	15.2
o-ZrRuP	orthorhombic	Co_2P-type	6.417	7.322	3.862	15.1
h-HfRuP	hexagonal	Fe_2P-type	6.414	—	3.753	14.9
ZrRuAs	hexagonal	Fe_2P-type	6.586	—	3.891	16.2
ZrRhSi	orthorhombic	Co_2P-type	6.549	7.459	3.918	16
h-ZrRuSi	hexagonal	Fe_2P-type	6.6838	—	3.6717	15.8
ZrRuGe	orthorhombic	TiFeSi-type	7.479	11.675	6.772	16.4
NbPS	orthorhombic	NbPS-type	3.443	11.919	4.733	16.1
$LaRu_4P_{12}$	cubic	$LaFe_4P_{12}$-type	8.0605	—	—	15.4

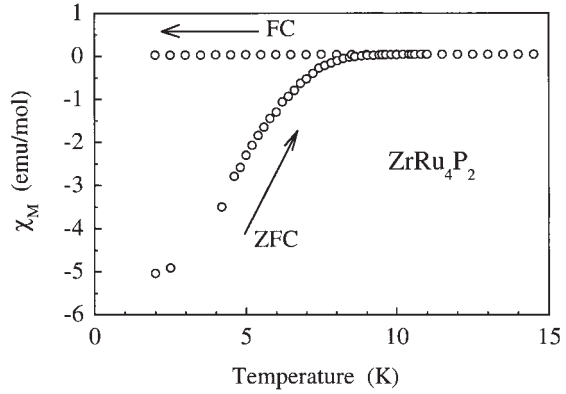

Fig. 4. Temperature dependence of dc magnetic susceptibility measured in an applied field of 5 *Oe* for the polycrystalline sample of $ZrRu_4P_2$.

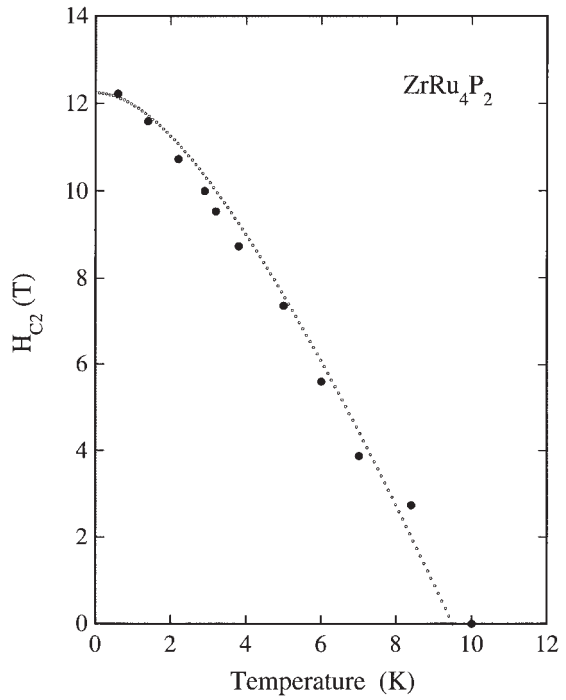

Fig. 5. H_{c2} vs temperature curve for $ZrRu_4P_2$; the dotted curve is fitted to the pair breaking model[31]; the open circles are T_c values measured by us.

value obtained from this data is 12.2 T at 0 K. The coherence length (ξ) of h-$ZrRu_4P_2$ can be estimated from the formula

$$H_{c2} = \Phi_0/2\pi\xi^2 \qquad (\Phi_0 = hc/2e) \tag{1}$$

The coherence length of the compound is 52 Å.

[2] MM′X Compounds with Fe_2P-, Co_2P- and TiFeSi-Type Structures. 1. ZrRuP and HfRuP: Researchers have prepared h- and o-ZrRuP at high temperatures and high pressures.[11] Temperature of preparation for o-ZrRuP is lower than that of h-ZrRuP at high pressure. The density of ZrRuP is 8.172 g/cm^3 for the orthorhombic form and 8.148 g/cm^3 for the hexagonal phase at room temperature under ambient pressure. These results suggest that the hexagonal form is a high temperature phase of ZrRuP. By use of synchrotron radiation, we have studied in situ X-ray diffraction of o-ZrRuP at

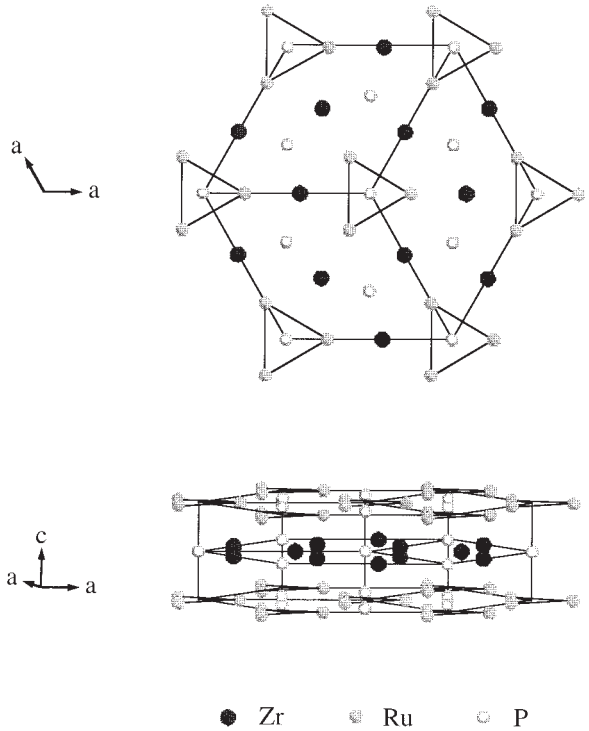

Fig. 6. Crystal structure of h-ZrRuP with a hexagonal Fe_2P-type form.

high temperatures and high pressures; this phosphide with the orthorhombic structure transforms to the hexagonal form at around 1100 °C under 3.5 GPa.[10] The h-ZrRuP that is quenched though the hexagonal form is the high-temperature phase.

Figure 6 shows the crystal structure of h-ZrRuP with the hexagonal Fe_2P-type form (C22, space group *P*-62*m*). Each layer in the hexagonal lattice is occupied by either Zr and P atoms or Ru and P atoms.[8] There are the Zr–Ru zig-zag chains along the c-axis in h-ZrRuP. The two-dimensional triangular clusters of Ru_3 are formed, and these are linked with each other through the Ru–P bonds in the basal plane. Two-dimensional triangular clusters of Ru_3s have a nearest-neighbor Ru–Ru distance of 2.63 Å, which is smaller than the average distance of 2.68 Å in the Ru metal. The shortest Ru–P distance (2.42 Å) almost agrees with the sum of the atomic radius of Ru (1.34 Å) and the covalent radius of P (1.06 Å). Figure 7 shows the crystal structure of o-ZrRuP with the orthorhombic Co_2P-type form (C23, space group *Pnam*). The structure of o-ZrRuP has layers that are filled with Zr, Ru and P atoms, and these layers are all equivalent.[9] The shortest Ru–P distance (2.398 Å) almost agrees with the sum of the atomic radius of Ru (1.34 Å) and the covalent radius of P (1.06 Å). There are no direct Ru–Ru and Zr–Zr connections between the layers in the hexagonal structure, but there are isoatomic zig-zag chains of Zr and Ru in the orthorhombic structure.

The stable oxidation states of Zr, Ru and P atoms are +4, +3 and −3, respectively. Seo et al. suggest that the bonding of ZrRuP can be described in terms of the oxidation states $Zr^{4+}(RuP)^{4-}$; $(RuP)^{4-}$ can be rewritten as $(Ru^{2-})(P^{2-})$ or $(Ru^{-})(P^{3-})$.[32] Especially, Ru in ZrRuP has some anomalous valence states.

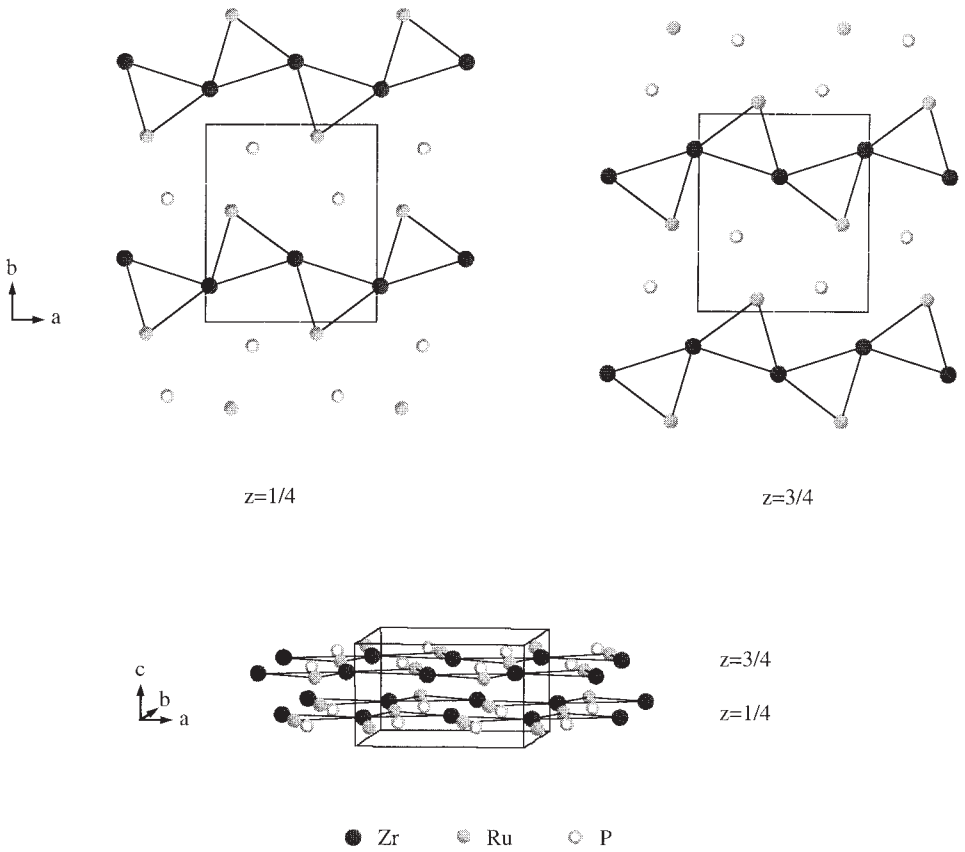

Fig. 7. Crystal structure of o-ZrRuP with an orthorhombic Co_2P-type form.

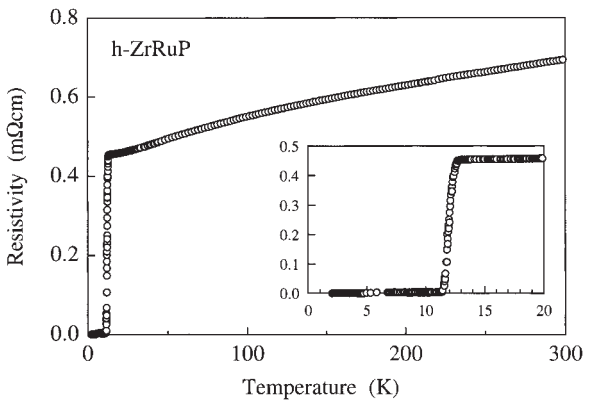

Fig. 8. Electrical resistivity of h-ZrRuP at low temperatures.

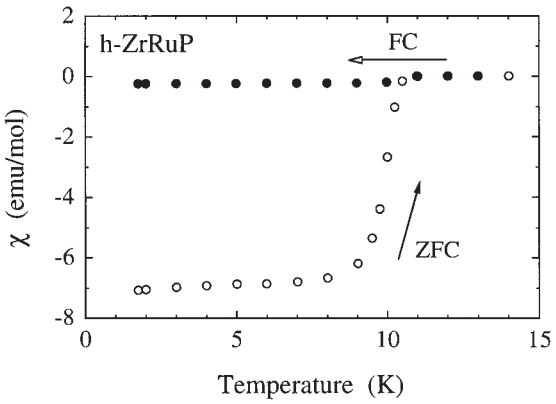

Fig. 9. Temperature dependence of dc susceptibility measured in an applied magnetic field of 5 *Oe* for h-ZrRuP.

Low frequency ac magnetic susceptibility of h-ZrRuP prepared by an arc-melted method were measured at low temperatures; the susceptibility rapidly decreases at around 13 K.[8] Figure 8 shows the temperature dependence of the electrical resistivity of h-ZrRuP prepared at high pressure. The resistivity of this phosphide slightly decreases with decreasing temperature, becoming zero at around 13 K. Figure 9 shows the temperature dependence of dc susceptibility measured in an applied magnetic field of 5 *Oe* for h-ZrRuP. The sample cooled in zero field shows a magnetic shielding equal to approximately 100% of that expected for perfect diamagnetism. The existence of hysteresis between zero-field cooling (ZFC) and field cooling (FC) indicates that the phosphide is a type II superconductor. The magnetic susceptibility of the coexistence phase of h- and o-ZrRuP prepared at high pressure has been studied at low temperatures; magnetic anomalies are found at around 4 and 11 K.[11] These are due to the superconducting transition for h- and o-ZrRuP. The T_c values of h-ZrRuP are much higher than that of o-ZrRuP.

According to the BCS theory,[33] the T_c of materials is related to the electronic density of states at the Fermi level [$D(E_F)$] and the electron-lattice interaction V as follows:

$$T_c = 1.14\Theta \exp[-1/VD(E_F)] \quad (2)$$

where Θ is the Debye temperature. Specific heat measure-

ments of h- and o-ZrRuP have already been carried out at low temperatures; the electronic density of states (DOS) at the Fermi energy [$D(E_F)$] is relatively low at 0.76 states/eV-atom and 0.72 states/eV-atom for h- and o-ZrRuP, respectively.[34,35] Seo et al. have calculated the electronic band structures of h- and o-ZrRuP with the extended Hückel tight-binding method; the $D(E_F)$ value at the Fermi level is 0.21 states/eV-atom for h-ZrRuP and 0.29 states/eV-atom for o-ZrRuP.[32] These values are considerably smaller than those obtained by the specific heat measurements of both phosphides. Recently, Hase has calculated the band structure of h-ZrRuP by the full-potential linearized augmented plane wave method within the local-density approximation.[36] The calculated density of states at the Fermi level (0.71 states/eV-atom) in h-ZrRuP is very close to the experimental result.

Stewart et al. have reported that the electron-phonon coupling parameter obtained from the specific heat measurement is 0.79 for h-ZrRuP[34] and 0.48 for o-ZrRuP.[35] The electron-phonon coupling of h-ZrRuP is larger than that of o-ZrRuP. The resistivity of both phosphides was measured at low temperatures and at high pressures.[37] T_c's of both compounds decrease with increasing pressure at the rate of -53 mK/GPa for h-ZrRuP and -98 mK/GPa for o-ZrRuP. These mainly arise from the change of the electron-phonon coupling parameter with pressure.[37] Seo et al. have pointed out that the electron-phonon coupling is important in making T_c higher for h-ZrRuP than for o-ZrRuP.[32]

Resistances of h-ZrRuP were measured as a function of the applied magnetic field at constant temperature and as a function of temperature at the constant magnetic field.[38] Figure 10 shows resistances of h-ZrRuP plotted as a function of temperature at constant magnetic fields between 0 and 14 T. The T_c value rapidly decreases with increasing the magnetic field. Figure 11 shows the H_{c2} vs temperature curve for h-ZrRuP. The temperature in which the resistance becomes zero is taken as T_c. The H_{c2}-temperature curve is fitted by the pair breaking model as shown by a dotted line.[31] The H_{c2} value obtained from this data is 16 T at 0 K. The coherence length of h-ZrRuP is 45.4 Å from Eq. 1. Electrical and magnetic properties of h-HfRuP have been studied at low temperatures.[8,11] H_{c2} and ξ values of this phosphide are 14 T and 48.5 Å, respectively.[38]

2. Alloys $ZrRu_{1-x}Rh_xP$ ($x = 0.01$, 0.05, 0.1, 0.15, 0.20, 0.25, 0.3, 0.4 and 0.5): Ru atom has one less valence electron than does Rh atom. ZrRhP with the Co_2P-type structure shows the superconducting transition at around 1.5 K.[9] The cell volume/formula unit of ZrRhP agrees with that of o-ZrRuP and is slightly smaller than that of h-ZrRuP. When the Ru atoms in h-ZrRuP are slightly displaced by the Rh atoms, the crystal structure changes drastically and the T_c value of the superconductivity is sharply suppressed.[39]

Figure 12 shows X-ray diffraction patterns of $ZrRu_{1-x}Rh_xP$ ($x = 0$, 0.01, 0.05, and 0.15) prepared at around 1300 °C and 4 GPa. The diffraction profile of ZrRuP ($x = 0$) shows the hexagonal Fe_2P-type structure at room temperature. The pattern of $ZrRu_{0.95}Rh_{0.05}P$ mainly indicates the orthorhombic Co_2P-type structure, though there are several weak lines of the hexagonal phase. Below $x = 0.15$, the hexagonal and orthorhombic phases coexist. The alloys of above $x = 0.2$ come very close to the single phase of the Co_2P-type structure. The structure of the alloys is very sensitive to the concentration of Rh atom. Figure 13 shows the phase diagram of the alloys $ZrRu_{1-x}Rh_xP$ prepared at high pressure. The stable region for the hexagonal phase is very small. Thus, Rh atoms dominate

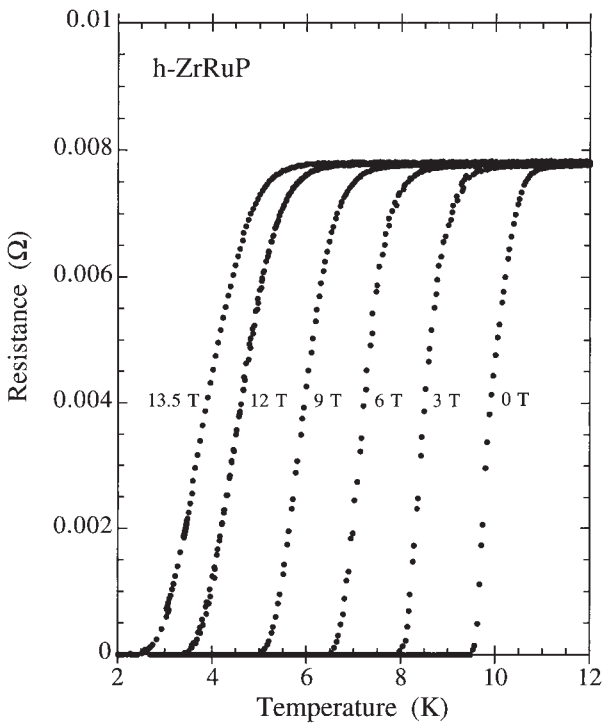

Fig. 10. Resistances of h-ZrRuP plotted as a function of temperature under the constant applied magnetic fields between 0 and 14 T.

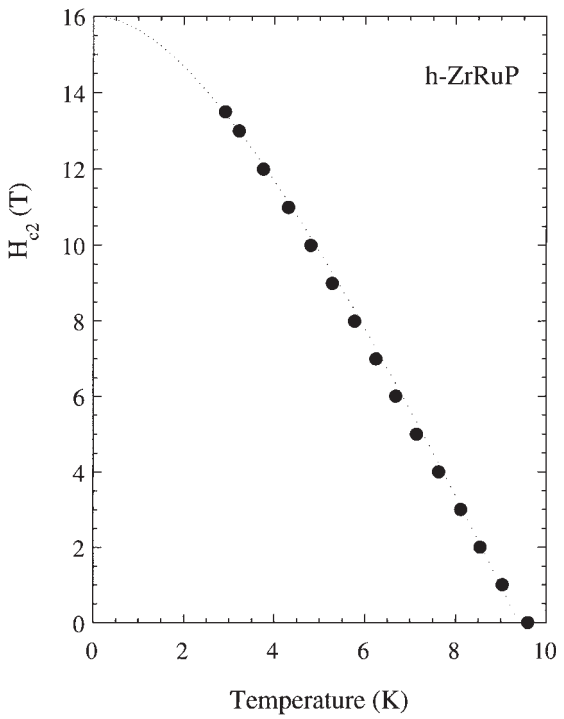

Fig. 11. H_{c2} vs temperature curve for h-ZrRuP.

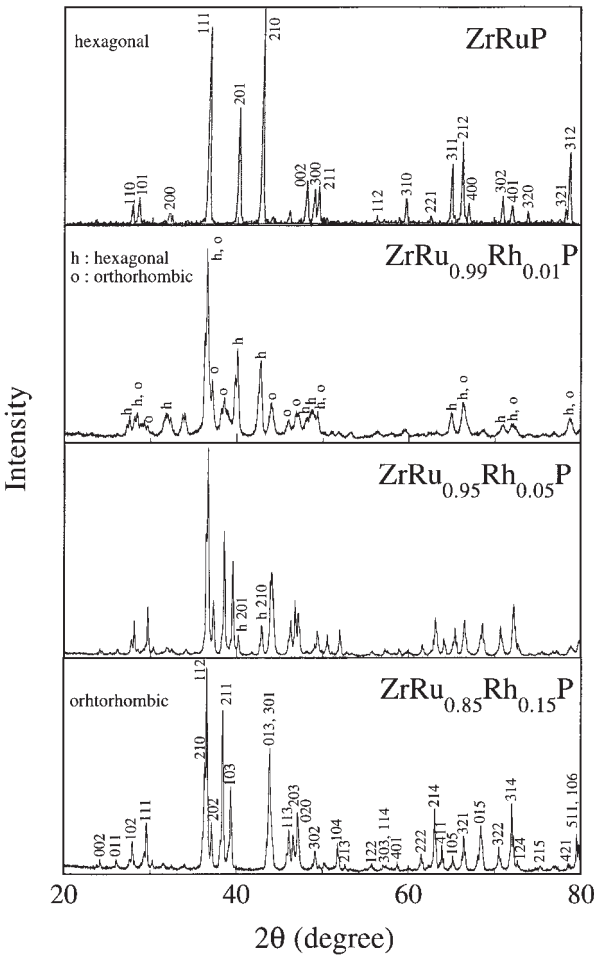

Fig. 12. X-ray diffraction patterns of $ZrRu_{1-x}Rh_xP$ ($x = 0$, 0.01, 0.05, and 0.15) prepared at around 1300 °C and 4 GPa.

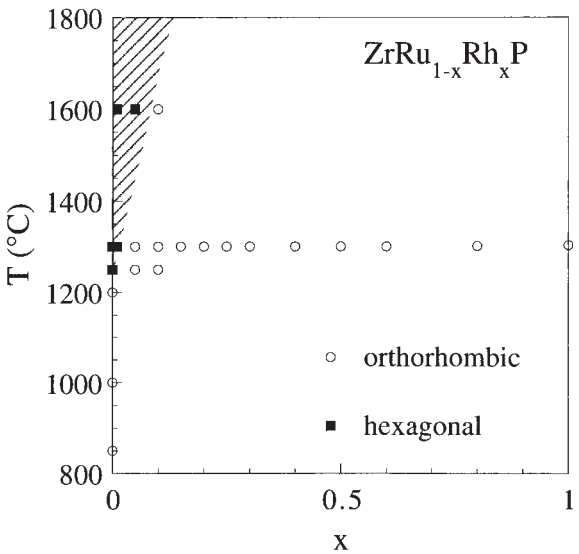

Fig. 13. Phase diagram of the alloys $ZrRu_{1-x}Rh_xP$ prepared at high pressure.

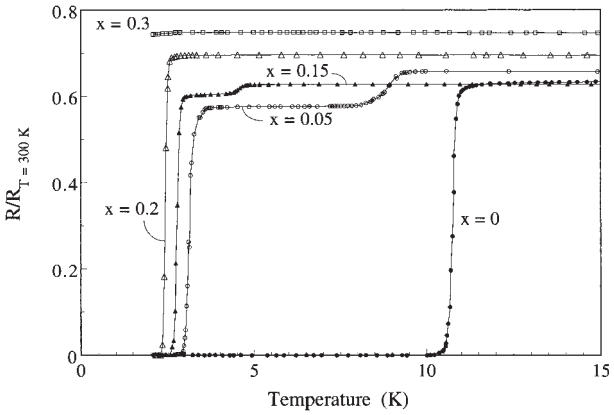

Fig. 14. Resistivity vs temperature curves for the alloys $ZrRu_{1-x}Rh_xP$ ($x = 0$, 0.05, 0.15, 0.2 and 0.3) prepared at around 1300 °C and 4 GPa.

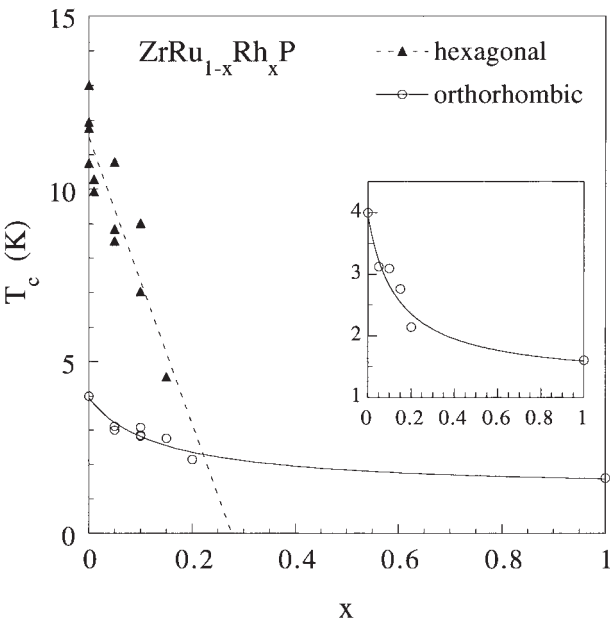

Fig. 15. T_c plotted as a function of x in the alloys $ZrRu_{1-x}Rh_xP$.

the structure of the alloys.

Figure 14 shows resistivity vs temperature curves for the alloys $ZrRu_{1-x}Rh_xP$ ($x = 0$, 0.05, 0.15, 0.2 and 0.3) prepared at around 1300 °C and 4 GPa. The alloys indicate the superconductivity between 2 and 12 K. Two electrical anomalies for $x = 0.05$, 0.1 and 0.15 are found in the resistivity-temperature curves. Both anomalies arise from the coexistence of the hexagonal and orthorhombic phases in the alloy. The alloy with $x = 0.2$ shows the superconductivity of the orthorhombic form only. The T_c values in the alloys above $x = 0.3$ become lower than 2 K, and must be close to the T_c (1.5 K) of ZrRhP. Figure 15 shows T_c plotted as a function of x in the alloys. T_c's of the hexagonal and orthorhombic phases of $ZrRu_{1-x}Rh_xP$ decrease rapidly with increasing x. Especially, T_c of the hexagonal phase of the alloys sharply decreases from 13 K at $x = 0$ to 4.5 K at $x = 0.15$. The Rh atoms suppress the T_c value of the superconductivity in the alloys.

The number of d electrons in a Rh atom is one more than that in a Ru atom. Thus, it is expected that the Fermi level in the alloys h-$ZrRu_{1-x}Rh_xP$ will rise with increasing x. If the band structure of h-ZrRuP is essentially not changed by the substitution of Rh atoms, DOS calculated near the Fermi level must increase with increasing x.[32,36] However, the experimental results show that the T_c value of the alloys rapidly decrease with increasing x. The anomalous suppression of T_c for the alloys cannot be explained by the change of $D(E_F)$. As the electron-phonon coupling parameter is large for h-ZrRuP, the change of the electron-phonon coupling may play an important role for T_c of the superconductivity of the alloys. Further, h-ZrRuP has a partially filled 1D band along the c direction.[32,36] The 1D chains along the c-axis in the alloys must be broken by the substitution of Rh atoms. We suggest that the anomalous suppression of T_c for the alloys mainly arises from the breaking of the 1D chains.[39]

3. ZrRuAs: Magnetic susceptibility of ZrRuAs prepared by the arc-melted method was already measured at low temperatures; ac susceptibility decreases sharply at around 11.9 K.[40] This arsenide has the hexagonal Fe_2P-type structure.[40] We prepared h-ZrRuAs at around 1300 °C and 4 GPa.[41] Figure 16 shows electrical resistivity vs temperature curves for h-ZrRuAs prepared at high pressure. The resistivity of this arsenide decreases slowly with decreasing temperature, and suddenly drops at around 11.5 K. This value almost agrees with the result of ac magnetic susceptibility measurements. The T_c of h-ZrRuAs is highest among the metal arsenides. Hase has calculated the band structure of h-ZrRuAs by the full-potential linearized augmented plane wave method within the local-density approximation.[36] The band structure of h-ZrRuAs is almost the same as that of isoelectronic h-ZrRuP. The main part of the $D(E_F)$ comes from the Ru4d component. The calculated density of states at the Fermi level for h-ZrRuAs is larger than that of h-ZrRuP. This arises from the difference of the Ru-Ru distance in the Ru_3 cluster. The nearest Ru–Ru distance is 2.63 Å for h-ZrRuP[8] and 2.80 Å for ZrRuAs.[40]

The magnetic field dependence of the resistance of h-ZrRuAs was measured at constant temperatures between 2 and 12 K.[38] The T_c decreases rapidly with increasing magnetic field. The H_{c2} value obtained from the H_{c2}–T curve is 14.1 T at 0 K. The coherence length of h-ZrRuAs is 48.3 Å.

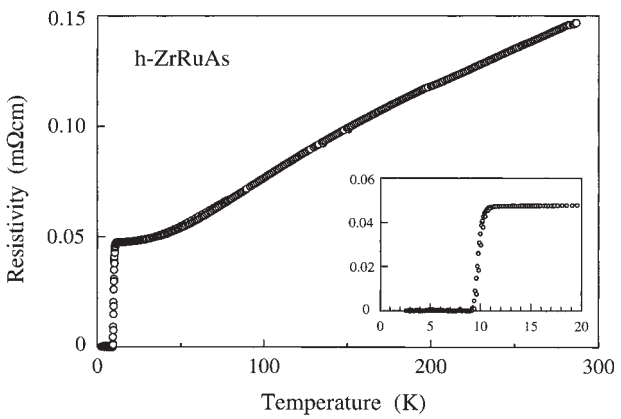

Fig. 16. Electrical resistivity vs temperature curve for h-ZrRuAs prepared at high pressure.

4. ZrRuSi: X-ray diffraction pattern of ZrRuSi prepared at around 1400 °C and 4 GPa agrees with that of h-ZrRuSi reported by Jonson and Jeitschko.[42] On the other hand, the X-ray diffraction profile of ZrRuSi prepared at around 950 °C and 4 GPa is similar to that of o-ZrRuP.[13] Thus, ZrRuSi also has two modifications: the Fe_2P- and Co_2P-type structures. The h-ZrRuSi is found to be isostructural to h-ZrRuP. The effect of replacing the phosphorus atom by the more electronegative silicon atom is an increase in the nearest-neighbor Ru–Ru distance to 2.87 Å.[42] The superconducting transition of h-ZrRuSi prepared at 1500 °C and 4 GPa was observed at around 12.2 K. The o-ZrRuSi prepared at lower temperatures showed the superconductivity at around 4 K.[13] ZrRuSi has one fewer valence electrons than does ZrRuP. The superconductivity observed in h-ZrRuSi is very interesting as ZrRuSi and ZrRuP are not isoelectronic compounds.

The shape of DOS near the Fermi energy for h-ZrRuSi is similar to those of h-ZrRuP and h-ZrRuAs. Since the Si3s and Si3p levels are higher than P3s and P3p respectively, these states are more hybridized with Ru4d and Zr4d states. The total $D(E_F)$ of h-ZrRuSi is 0.48 states/eV-atom, which is about a half of that of h-ZrRuP.[36] However, this value is larger than the result obtained by Seo et al.[32]

The magnetic field dependence of the resistance for h-ZrRuSi was measured at constant temperatures. Figure 17 shows the resistances of h-ZrRuSi plotted as a function of the applied magnetic field at constant temperatures between 2 and 12 K. The T_c decreases rapidly with increasing the applied magnetic field. The H_{c2} value of h-ZrRuSi is 14.5 T at 0 K. The coherence length of h-ZrRuSi is 47.7 Å.[38]

5. MRhSi with Co_2P-Type Structure (M = Ti, Zr and Hf): The T_c's values of many ternary metal compounds with the Co_2P-type structure are between 2 and 5 K.[9,43] As mentioned above, the compounds with the Fe_2P-type structure have the T_c values of above 10 K. The Fe_2P-type structure seems to be favorable for the enhancement of superconductivity. However, we have found that ZrRhSi with the Co_2P-type structure has a T_c above 10 K.[44] Figure 18 shows

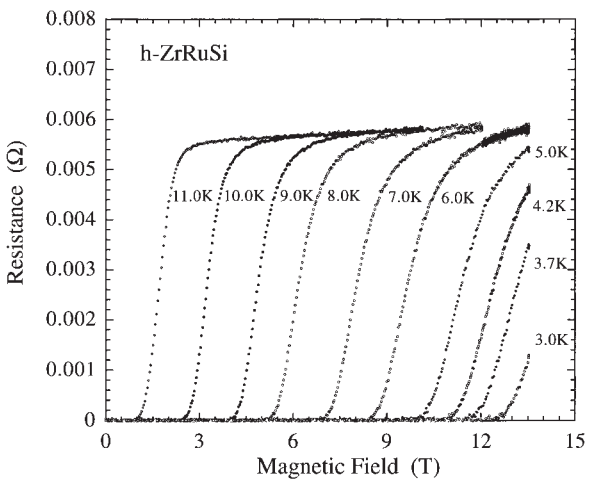

Fig. 17. Resistances of h-ZrRuSi plotted as a function of the applied magnetic field at constant temperatures between 2 and 12 K.

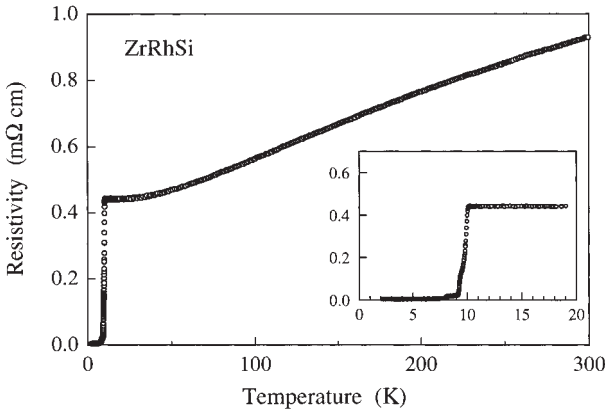

Fig. 18. Resistivity vs temperature curve for o-ZrRhSi prepared at around 1600 °C and 4 GPa.

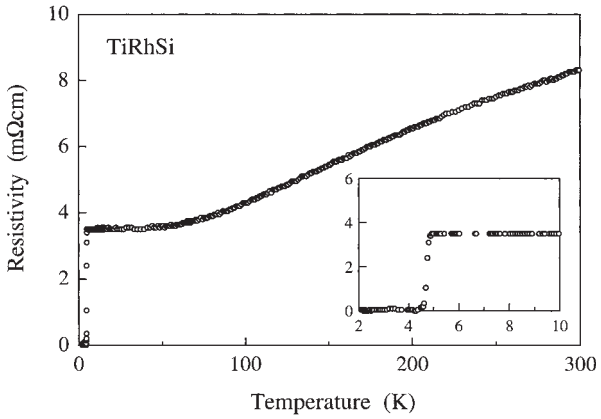

Fig. 19. Resistivity of TiRhSi plotted as a function of temperature.

resistivity vs temperature curves for ZrRhSi prepared at around 1600 °C and 4 GPa. The superconducting transition of ZrRhSi was observed at around 10.3 K. ZrRhSi and ZrRuP are isoelectronic compounds with the valence electrons/formula unit of 17. Further, ZrRhSi is isostructural to o-ZrRuP. As o-ZrRuP does not possess a partial 1D band, its T_c is low.[32] However, the T_c of ZrRhSi is much higher than that of o-ZrRuP, comparable to that of h-ZrRuP. We suggest that $D(E_F)$ of ZrRhSi is larger than that of o-ZrRuP because the Si3s and Si3p level are easily hybridized with Ru4d and Zr4d states.

Figure 19 shows the resistivity of TiRhSi plotted as a function of temperature. The resistivity vs temperature curve of TiRhSi is very similar to that of ZrRhSi. The superconducting transition of the compound was observed at around 5 K. The dc susceptibility vs temperature curve for TiRhSi was measured in an applied field of 5 *Oe*. Susceptibility of the silicide decreases sharply at around 5 K.[44] The T_c of h-TiRuP with the Fe_2P-type structure is below 1.5 K.[8] This is much lower than that of TiRhSi with the Co_2P-type structure. Generally speaking, the T_c of the compounds with the Fe_2P-type structure is much higher than that of the compounds with the Co_2P-type structure. Thus, the low T_c value of h-TiRuP is quite puzzling.[8]

6. ZrRuGe: The X-ray diffraction pattern of ZrRuGe

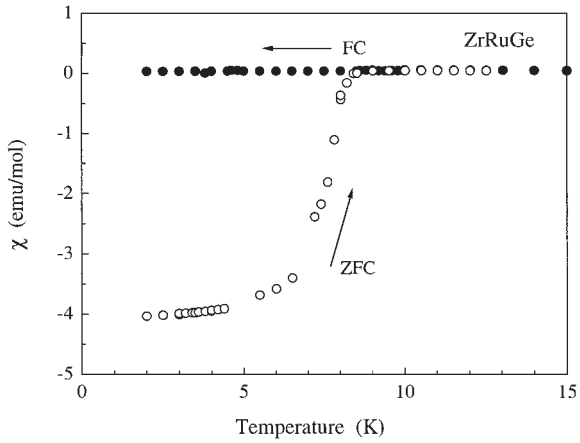

Fig. 20. Temperature dependence of dc magnetic susceptibility measured in an applied field of 5 *Oe* for the polycrystalline sample of ZrRuGe.

resembles that of h-ZrRuSi. However, some diffraction lines are broadened or split, there are also same additional lines which cannot be indexed with the Fe_2P-type structure. This pattern is indexed with the orthorhombic TiFeSi-type structure.[45] Figure 20 shows the temperature dependence of the dc magnetic susceptibility measured in an applied field of 5 *Oe* for the polycrystalline sample of ZrRuGe. The existence of hysteresis between zero-field cooling and field cooling indicates that the germanide is a type II superconductor.[38,46] The superconductivity of several equiatomic ternary germanides has been studied; T_c's of these compounds are between 2 and 5 K.[47] ZrRuGe has the highest T_c among the ternary metal germanides.

Seo et al. have pointed out that h-ZrRuP has a nearly half-filled one-dimensional (1D) band along the c direction. A CDW instability associated with a 1D band is a likely cause for the occurrence of change from the h-MM′X (M and M′: transition metal, Fe_2P-type structure) to o′-MM′X ("dimerized" form of h-MM′X, TiFeSi-type structure) in HfRuAs and TiRuAs phases. h-ZrRuP does not undergo a distortion from h-MM′X to o′-MM′X because the CDW instability is not strong enough. However, this instability appears to provide soft phonons conductive to superconductivity, leading to a high T_c value for h-ZrRuP.[32] However, we have found that o′-ZrRuGe with the TiFeSi-type structure shows the superconductivity at around 10.5 K.[38,46] As the high T_c value of ZrRuGe cannot be explained by their theory,[32] this germanide is a very interesting superconductor.

The resistance of ZrRuGe was measured as a function of the applied magnetic field at constant temperatures between 2 and 10 K. The H_{c2} value obtained from this data is 8.3 T at 0 K. The coherence length of ZrRuGe is 63.0 Å.[38]

7. MM′P (M = Mo and W; M′ = Ni and Ru): MoNiP and WNiP have the hexagonal Fe_2P-type structure.[48] On the other hand, MoRuP and WRuP take the orthorhombic Co_2P-type structure.[49] Recently, the crystal structure of MoRuP was refined by the Rietveld analysis using powder X-ray diffraction data.[50] Figure 21 shows the electrical resistivity vs temperature curves for MoRuP prepared at around 1600 °C and 4 GPa. The resistivity sharply drops at around 15.5 K.[12] The dc mag-

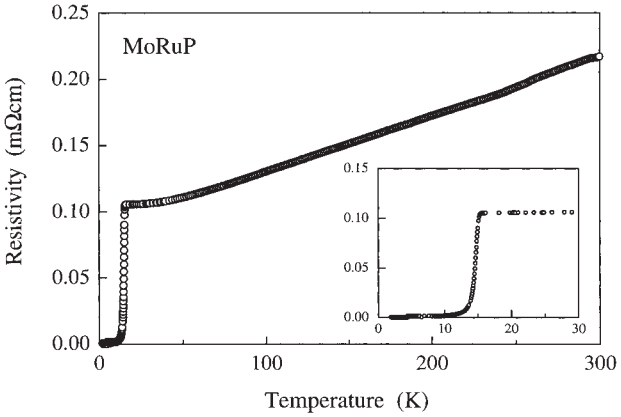

Fig. 21. Electrical resistivity vs temperature curve for MoRuP prepared at around 1600 °C and 4 GPa.

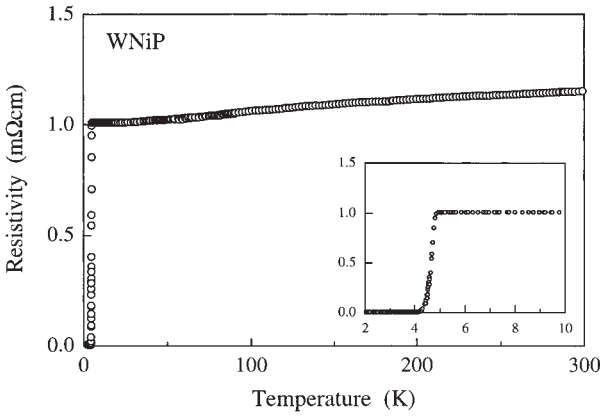

Fig. 22. Electrical resistivity vs temperature curve for WNiP prepared at around 1600 °C and 4 GPa.

netic susceptibility sharply decreases at around 15 K and 4 K. The magnetic anomaly at around 4 K may be due to some impurity based on the binary molybdenum phosphides. The superconductivity of the binary molybdenum phosphides prepared at high pressures is observed at around 7 K for Mo_3P, 5.8 K for Mo_8P_5 and 3 K for Mo_4P_3.[51] Mo_3P has the highest T_c value in the binary metal phosphides. When the ternary molybdenum phosphide is prepared at high pressures, a small amount of the binary molybdenum phosphide also is produced. Thus, the binary phosphides act as the impurity.

The electrical and magnetic properties of MoNiP are similar to those of MoRuP at low temperatures. MoNiP shows the superconducting transition at around 15.5 K.[52] The T_c value of MoNiP and MoRuP is highest among the metal phosphides.

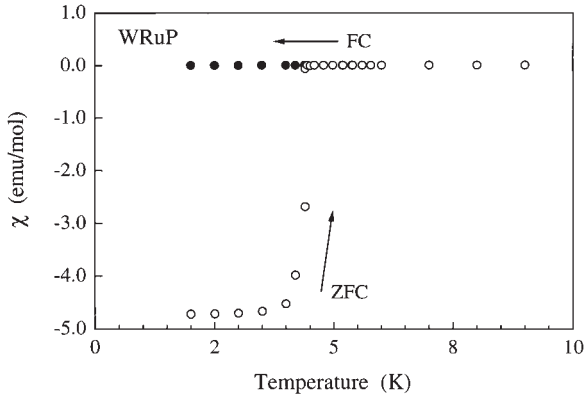

Fig. 23. Temperature dependence of dc magnetic susceptibility measured in an applied field of 5 *Oe* for the polycrystalline sample of WRuP.

Figure 22 shows electrical resistivity vs temperature curves for WNiP prepared at around 1600 °C and 4 GPa. The resistivity of the wolfram compound sharply decreases at around 5 K. Figure 23 shows the temperature dependence of dc magnetic susceptibility measured in an applied field of 5 *Oe* for the polycrystalline sample of WRuP. The dc magnetic susceptibility of the compound abruptly decreases at around 5 K. Similar magnetic behavior is also observed for WNiP prepared at high pressure.

The T_c and crystal data of MRuP and MNiP (M = Mo or W) are summarized in Table 3. The T_c of h-ZrRuP and h-HfRuP with 4d or 5d transition metal is about 13 K. NbRhP and TaRhP with 4d or 5d transition metal have almost the same T_c. A replacement of the early 4d transition metal by the 5d element causes only a small change in the T_c in each structure for these superconductors. However, when molybdenum atoms are replaced by wolfram atoms, the T_c decreases sharply from 15.5 K to 5 K. The T_c of the molybdenum compounds is three times higher than that of the wolfram phosphides. This relationship is also found for the binary metal phosphides. The T_c value of Mo_3P (T_c = 7 K) is about three times that of W_3P (T_c = 2.26 K).[53] These results suggest that the electronic states in the vicinity of the Fermi level are mostly composed of the 4d or 5d orbitals of the molybdenum or wolfram atoms in MRuP and MNiP. NMR measurements in MoNiP have been carried out at low temperatures. The electronic density of states at the Fermi level has the Mo4d character and its

Table 3. T_c and Crystal Data of MRuP and MNiP (M = Mo or W)

	MoNiP	WNiP	MoRuP	WRuP
Valence electrons/formula unit	21	21	19	19
Structure	hexagonal Fe_2P-type	hexagonal Fe_2P-type	orthorhombic Co_2P-type	orthorhombic Co_2P-type
a/Å	5.858(1)	5.8614(6)	6.035(1)	5.9791(4)
b/Å	—	—	6.9935(9)	6.9325(7)
c/Å	3.668(1)	3.6072(6)	3.8572(5)	3.8726(6)
Cell volume/formula unit (Å^3)	36.35	35.77	40.4	40.13
c/a	0.626	0.615	0.639	0.648
T_c/K	15.5	4.9	15.5	5.5

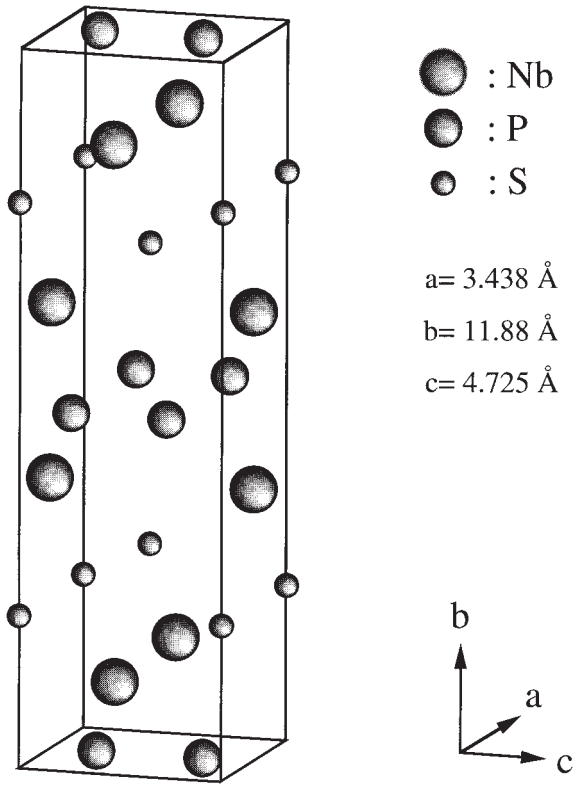

Fig. 24. Crystal structure of NbPS.

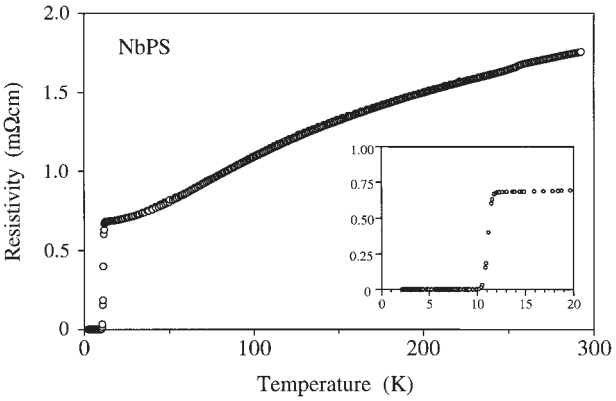

Fig. 25. Resistivity vs temperature curve for NbPS prepared at around 1300 °C and 5 GPa.

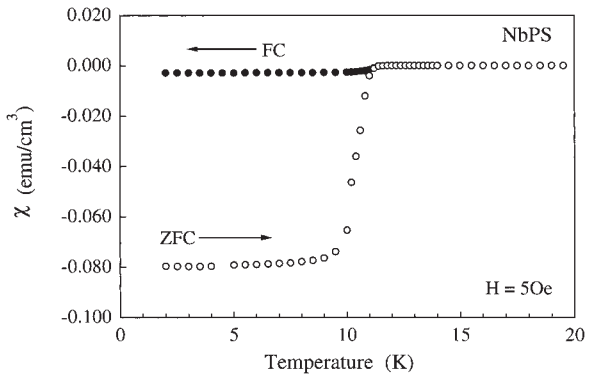

Fig. 26. Temperature dependence of dc magnetic susceptibility measured in an applied field of 5 *Oe* for the polycrystalline sample of NbPS.

weight is considerably large.[54] MoRuP is isostructural to o-ZrRuP. However, T_c of MoRuP (15.5 K) is much higher than that of o-ZrRuP (4 K). The shortest Zr–P distance (2.742 Å) in o-ZrRuP is much longer than the shortest Mo–P spacing (2.44 Å) in MoRuP. The bonding in MoRuP must differ from that in o-ZrRuP.[50] MoNiP with the Fe_2P-type structure has the Mo–P distance which is short compared with the Zr–P distance in h-ZrRuP. The main part of the $D(E_F)$ for ZrRuP comes from the Ru4d component.[32,36] On the contrary, the $D(E_F)$ values of both Mo compounds mainly arise from Mo4d component. This difference between Zr and Mo compounds may be closely related to the superconducting properties.

ZrRhSi and MoRuP with the Co_2P-type structure and ZrRuGe with the TiFeSi-type structure show rather high T_c values of above 10K, though they do not have the one-dimensional chains like the compounds with the Fe_2P-type structure. These results suggest that the two-dimensional planar framework is quite important to the superconducting properties of equiatomic compounds.

[3] Non-Metal-Rich Compound NbPS. The interesting ternary niobium compound NbPS was prepared at high temperatures and high pressures. The compound is metallic, transforming to a superconductor at around 12 K.[14,15] Figure 24 shows the crystal structure of NbPS. This is the orthorhombic structure with space group *Immm*. There are several interesting features in the structure. The Nb atoms are eightfold coordinated by four P and four S atoms at the corners of a bicapped trigonal prism.[14] The prisms share faces, resulting in the formation of Nb–Nb dimers. The inter-atomic distance of 2.93 Å in the Nb–Nb dimers is in agreement with the sum obtained from the atomic radii. The S atoms are coordinated by four Nb atoms at the corners of a distorted tetrahedron, while the P atoms form continuous strings in the c-axis direction with alternating short (2.22 Å) and long (2.51 Å) distances. The short distances are similar to the lengths of the normal P–P covalent bonds found in many phosphides. Keszler and Hoffmann carried out the tight-binding band calculations for NbPS.[16]

Figure 25 shows the resistivity vs temperature curves for NbPS prepared at around 1300 °C and 5 GPa. The resistivity decreases with decreasing temperature, and sharply drops at around 12 K. Figure 26 shows the temperature dependence of the dc magnetic susceptibility measured in an applied field of 5 *Oe* for the polycrystalline sample of NbPS. The existence of hysteresis between zero-field cooling and field cooling indicates that the compound is a type Ⅱ superconductor. The susceptibility of NbPS is essentially temperature-independent in the region 10–300 K. This is indicative of Pauli paramagnetism and is consistent with metallic behavior, which is expected from the temperature dependence of the resistivity.

Figure 27 shows the result of the specific heat measurement on NbPS at low temperatures. The heat capacity (C) of the compound can be fitted to the expression $C = \gamma T + \beta T^3$ using a least squares analysis, which yields the values $\gamma = 6.5$ mJ mol^{-1} K^{-2} and $\beta = 0.16$ mJ mol^{-1} K^{-4}. In the normal state, $T > T_c$, the coefficient γ is related to the electronic density of states at the Fermi energy, $D(E_F)$, by

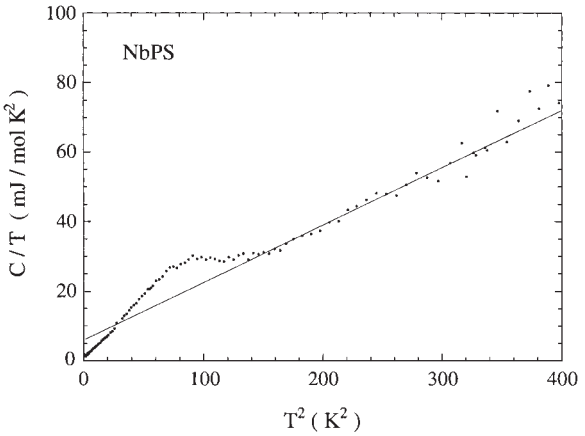

Fig. 27. Specific heat of NbPS at low temperatures.

$$\gamma = (\pi^2/3)nN_0{k_B}^2D(E_F)(1 + \lambda) \quad (3)$$

where n is the number of atoms per formula unit, N_0 is Avogadro's number, k_B is the Boltzmann constant, and λ is the electron-phonon coupling parameter given by McMillan.[55] The coefficient β is related to the Debye temperature(Θ) as

$$\beta = (12/5)\pi^4 nN_0k_B/\Theta^3 \quad (4)$$

Using the above data, we calculated the Debye temperature of NbPS as 330 K.

In order to derive $D(E_F)$, one may use McMillan's formula for λ,[55]

$$\lambda = [1.04 + \mu^* \ln(\Theta/1.45T_c)]/[(1 - 0.62\mu^*) \times \ln(\Theta/1.45T_c) - 1.04] \quad (5)$$

Here μ^* was taken to be 0.1.[34,35] Values of λ and $D(E_F)$ for NbPS were found to be 0.81 for λ and 0.51 states/eV-atom for $D(E_F)$. The density of states at the Fermi level found for NbPS is low, though T_c is relatively high.

Superconducting parameters of NbPS, h-ZrRuP and o-ZrRuP are summarized in Table 4. The values of $D(E_F)$ are 0.76 states/eV-atom for h-ZrRuP and 0.74 states/eV-atom for h-HfRuP.[34] $D(E_F)$ in NbPS is smaller than that of h-ZrRuP, though the T_c values of the two compounds are almost the same. The high T_c of NbPS may mainly arise from the strong electron-phonon coupling. ZrRuP is a metal-rich compound and NbPS is a non-metal-rich compound. However, the H_{c2} value of NbPS (17 T) is close to that of h-ZrRuP (16 T). This result suggests that the band structure of both compounds near the Fermi level is mostly d-orbital in character.

Table 4. Superconducting Parameters for h-ZrRuP, o-ZrRuP and NbPS

	h-ZrRuP	o-ZrRuP	NbPS
Density (g/cm^3)	8.148	8.172	5.37
T_c/K	13	4	13
Debye temperarure Θ_D/K	345	454	330
Electron-phonon coupling parameter λ	0.79	0.48	0.81
Density of states $D(E_F)$ [states/eV-atom]	0.76	0.72	0.51

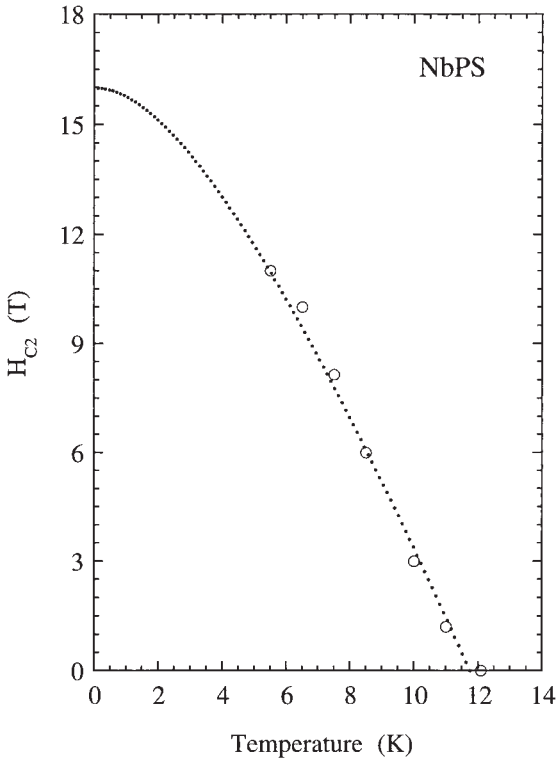

Fig. 28. H_{c2} vs temperature curve for NbPS.

As phosphorus atoms in NbPS form continuous strings along the c-axis with alternating short and long distances, and the short distances are in agreement with that expected of normal P–P covalent bonds, and if it is assumed that only phosphorus atoms separated by the short distance are bonded, then the valences in NbPS can be regarded as being $2Nb^{4+}$, $(P_2)^{4-}$ and $2S^{2-}$. Since Nb–Nb dimers with a d^1 electron configuration would be formed in the NbPS structure, the semiconductive behavior would be anticipated, as is found in NbI_4, where Nb–Nb dimers in the linear chain structure behave as a semiconductor.[56,57] However, in the case of NbPS, as the long P–P distances contain some bonding character, the valence of Nb must be lower, being somewhere between Nb^{4+} and Nb^{3+}.[14] Thus, NbPS can become metallic. Keszler and Hoffmann performed tight binding band structure calculations for NbPS.[16] The bands of NbPS near the Fermi level are mostly of Nb d orbital character and below this level they have P and S character. The d_{yz} band is flat over a large portion of the Brillouin zone, affording a peak in the density of states at the Fermi level. The presence of this band may be closely related to the superconductivity.

The magnetic field dependence of the resistance of NbPS has been studied at low temperatures. Figure 28 shows the H_{c2} vs temperature curve for NbPS. The H_{c2} value obtained from this data is 17 T at 0 K. This is the highest H_{c2} among the phosphide superconductors.[15]

[4] Filled Skutterudites MM'_4X_{12} (M and M′ = Metal, X = Pnicogen). Ternary metal pnictides with the general formula MM'_4X_{12} (M = lanthanide; M′ = Fe, Ru and Os; X = pnicogen) crystallize in a skutterudite ($CoAs_3$-type) structure filled by lanthanide atoms.[17–19] Figure 29 shows the filled skutterudite-type structure. M atoms located at (000) and

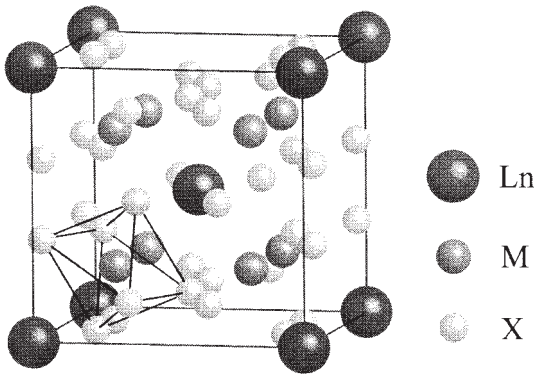

Fig. 29. Crystal structure of the filled skutterudites LnM_4X_{12} (Ln = lanthanide, M = transition metal, X = pnicogen).

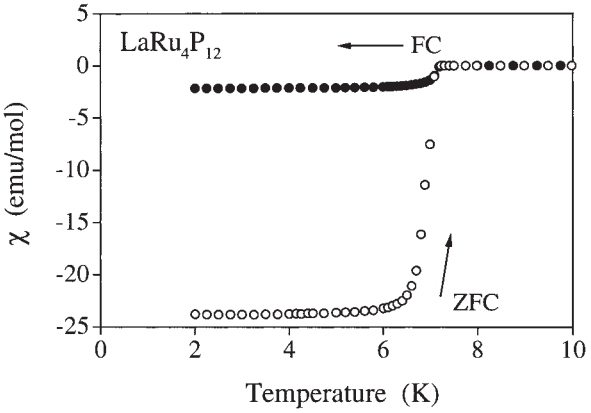

Fig. 30. Temperature dependence of dc susceptibility measured in an applied magnetic field of 5 *Oe* for $LaRu_4P_{12}$.

(1/2 1/2 1/2) of a cubic structure like bcc. The transition-metal atoms (M′) are in the center of a distorted octahedral environment of six pnicogen atoms. The skutterudite-type structure is characterized by formation of well defined X_4^{4-} groups. The filled skutterudites show interesting superconductivity aspects at low temperatures.[23,25,26]

Figure 30 shows the temperature dependence of dc susceptibility measured in an applied magnetic field of 5 *Oe* for $LaRu_4P_{12}$. Susceptibility sharply decreases at around 7 K. The sample cooled in zero field shows a magnetic shielding equal to approximately 100% of that expected for perfect diamagnetism.[58] The existence of hysteresis between zero-field cooling and field cooling indicates that $LaRu_4P_{12}$ is a type II superconductor. As the susceptibility is essentially temperature independent in the region of 7–300 K, the magnetic property of the phosphide is due to the Pauli paramagnetism. Figure 31 shows the results of the specific heat measurements of $LaRu_4P_{12}$ at low temperatures. The heat capacity C can be fit to the expression $C = \gamma T + \beta T^3$ by a least squares analysis, which yields the value $\gamma = 26.0$ mJ mol^{-1} K^{-2} and $\beta = 0.372$ mJ mol^{-1} K^{-4}, the latter value corresponding to the Debye temperature $\Theta = 446$ K. Since the specific-heat jump ΔC is 270 mJ mol K at T_c (= 7.0 K), $\Delta C/\gamma T_c$ is 1.48. This value almost agrees with 1.43 obtained by BCS theory. From Eqs. 3, 4 and 5, the values of λ and

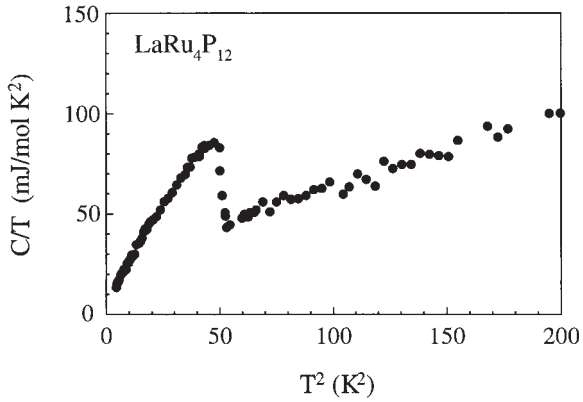

Fig. 31. Specific heat of $LaRu_4P_{12}$ at low temperatures.

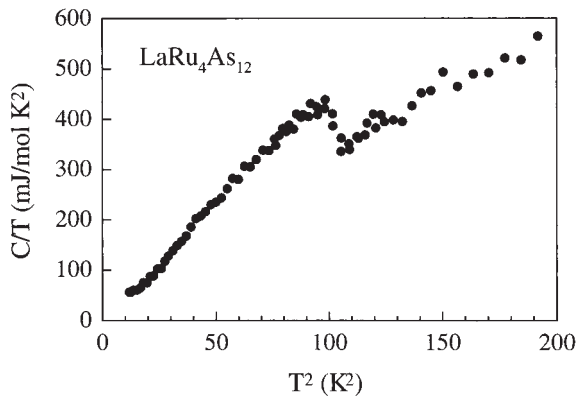

Fig. 32. Specific heat of $LaRu_4As_{12}$ at low temperatures.

$D(E_F)$ for $LaRu_4P_{12}$ are obtained as 0.56 and 0.42 states/eV-atom, respectively. According to the BCS theory, the superconducting electronic specific heat C_{es} of $LaRu_4P_{12}$ can be fit to the expression

$$C_{es}/\lambda T_c = 11.15 \exp(-1.72 T_c/T) \quad (6)$$

Since Δ (half of the energy gap) at around T_c is $1.72 k_B T_c$, $2\Delta/k_B T_c$ is 3.43. This value almost agrees with the value 3.53 obtained from BCS theory. The energy gap (2Δ) of $LaRu_4P_{12}$ is 2.13 meV.[58]

Figure 32 shows the result of the specific heat measurements of $LaRu_4As_{12}$ at low temperatures. From the temperature dependence of the heat capacity of the compound, we obtained the values $\gamma = 73$ mJ mol^{-1} K^{-2} and $\Theta = 233$ K.[23] Since the specific-heat jump ΔC is 1290 mJ mol^{-1} K^{-1} at T_c (= 10.1 K), $\Delta C/\gamma T_c$ is 1.75. This value is slightly larger than the value 1.43 obtained from BCS theory. The values of λ and $D(E_F)$ for $LaRu_4As_{12}$ are 0.86 and 0.98 states/eV-atom, respectively. The parameters obtained from the measurement of the heat capacity for $LaRu_4X_{12}$ (X = P and As) are summarized with results of $LaFe_4P_{12}$ reported by Meisner et al.[59] in Table 5. Both values of $LaRu_4As_{12}$ are larger than those of $LaRu_4P_{12}$. Thus, the T_c value of the arsenide becomes higher compared with that of the phosphide.

Figure 33 shows the resistivity of $LaRu_4As_{12}$ at low temperatures and at high pressures. The resistivity was measured using a cubic press under hydrostatic conditions.[60] The superconducting transition of this arsenide is observed at around

Table 5. Lattice Constant and Superconducting Parameters for LaT_4X_{12} (T = Fe, Ru; X = P and As)

	$LaFe_4P_{12}$[a)]	$LaRu_4P_{12}$	$LaRu_4As_{12}$
a/Å	7.8316	8.0605	8.5097
T_c/K	4.1	7.2	10.3
γ (mJ/mol·K^2)	57	26	73
Θ_D/K	580	446	233
$D(E_F)$ [states/eV-atom]	0.98	0.42	0.98
λ	0.45	0.57	0.86
$\Delta C/\gamma T_c$	1.25	1.48	1.75

a) Ref. 59.

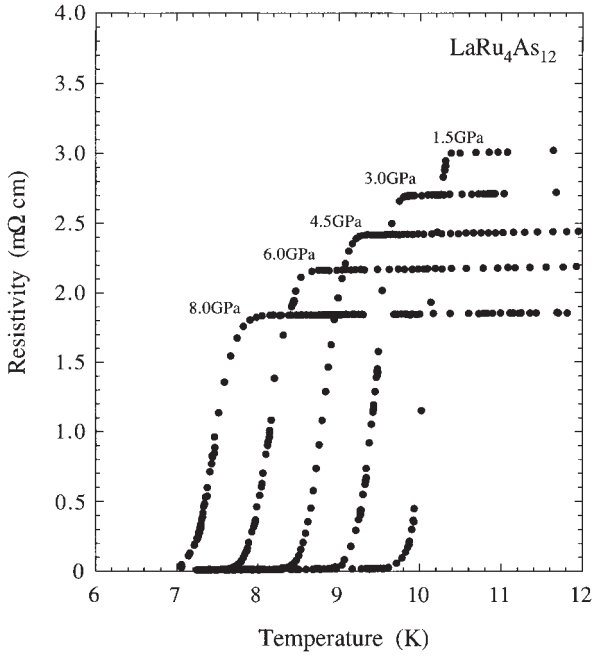

Fig. 33. Resistivity vs temperature curves for $LaRu_4As_{12}$ at high pressures.

10.3 K under ambient pressure. The T_c of the arsenide linearly decreases with increasing pressure at the rate of $dT_c/dP = -0.4$ K/GPa up to 8 GPa.[61] This value is much larger than the pressure shift of ZrRuP.[37] T_c's of several Cu–O-based high-temperature superconductors strongly depend on the pressure.[60] This result suggests that the electronic states near the Fermi level in $LaRu_4As_{12}$ are not as sensitive to pressure as the oxide superconductors.

The resistivity and the dc magnetic susceptibility of $LaOs_4As_{12}$ have been measured at low temperatures.[61] This arsenide shows a superconducting transition at around 3.2 K. On the contrary, the T_c of $LaOs_4P_{12}$ is 1.8 K. T_c's of $LaRu_4As_{12}$ and $LaOs_4As_{12}$ are high compared with those of the corresponding phosphides. The band electronic structure of $LaFe_4P_{12}$ has been calculated by employing the tight-binding method within the extended Hückel framework;[62] the major contribution to the highest occupied band of the phosphide comes from the orbitals of the P_4 rings that form the phosphorus sublattice. If phosphorus atoms in the skutterudite compounds are substituted by arsenic atoms, the electronic states of the metal arsenides must change significantly in the vicinity

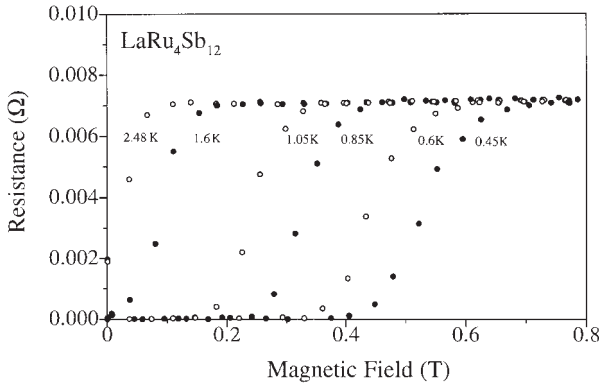

Fig. 34. Resistances of $LaRu_4Sb_{12}$ plotted as a function of the applied magnetic field at constant temperatures between 0.4 and 3 K.

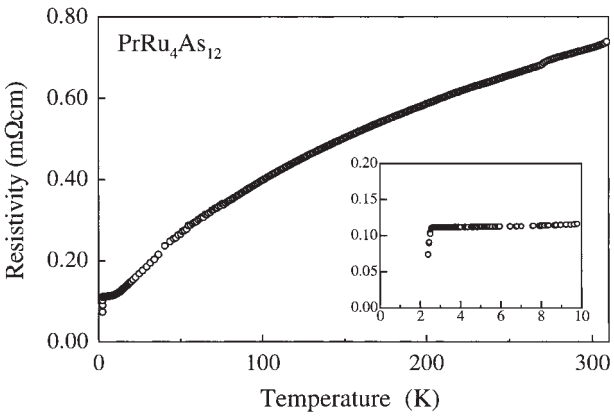

Fig. 35. Resistivity vs temperature curve for $PrRu_4As_{12}$.

of the Fermi level. The results of the specific heat show that $D(E_F)$ of $LaRu_4As_{12}$ is much larger than that of $LaRu_4P_{12}$. The magnitudes of density of states and electron-phonon coupling of the arsenides are larger than those of the phosphides.[58] Arsenic atoms play an important role for the enhancement of superconductivity in $LaRu_4As_{12}$ and $LaOs_4As_{12}$.

Figure 34 shows the resistances of $LaRu_4Sb_{12}$ plotted as a function of the applied magnetic field at constant temperatures between 0.4 and 3 K. The resistance rapidly decreases at around 2.8 K. The T_c decreases with increasing applied magnetic field. The superconducting transition of the compound becomes broader at low temperatures. The H_{c2} obtained from this data is 0.46 T at 0 K. The coherence length of the compound is 266 Å.[33] Similar resistance measurements for $LaRu_4P_{12}$ and $LaRu_4As_{12}$ were already carried out under the applied magnetic field. The H_{c2} value and the coherence length at 0 K are 3.65 T and 95 Å for $LaRu_4P_{12}$,[63] 0.72 T and 206 Å for $LaRu_4As_{12}$.[58] These values are larger than those of $LaRu_4Sb_{12}$.

Figure 35 shows the resistivity vs temperature curves for $PrRu_4As_{12}$. The resistivity drops sharply at around 2.4 K. The large diamagnetic susceptibility is observed at around 2.4 K.[23] These behaviors are due to the superconducting transition. On the contrary, we have found a metal-to-insulator transition at around 60 K for $PrRu_4P_{12}$.[24] The resistivity of the phosphide decreases with decreasing temperature from 300 K

Table 6. Number of Valence Electrons per Formula Unit, T_c, H_{c2} and Coherence Length for Superconducting Materials with T_c above 10 K

	Valence electrons / fomula unit	T_c/K	H_{c2}/T	Coherence length/Å
$ZrRu_4P_2$	46	11	12.2	52.0
h-ZrRuP	17	13	16	45.4
h-HfRuP	17	12.7	14	48.5
ZrRuAs	17	12	14.1	48.3
ZrRhSi	17	10.3	—	—
h-ZrRuSi	16	12.2	14.5	47.7
ZrRuGe	16	10.5	8.3	63.0
NbPS	16	13	17	44.0
$LaRu_4As_{12}$	75	10.3	0.72	206.0

to 60 K, and abruptly increases with decreasing temperature below 60 K. The structural phase transition in this phosphide was observed at around 60 K.[64] $PrFe_4P_{12}$ shows unusual heavy fermion behavior.[65] $PrFe_4P_{12}$ and $PrOs_4P_{12}$[24] do not show any superconductivity at low temperatures. Thus, $PrRu_4As_{12}$ is a new superconductor with a magnetic rare earth in a skutterudite compound. Recently, interesting superconductivity in $PrOs_4Sb_{12}$ has been observed at around 1.85 K.[25,26] This compound behaves as a heavy fermion superconductor with strongly correlated electrons.

One of the most striking features in filled skutterudites is the occurrence of the superconductivity for $LaFe_4P_{12}$ with T_c of 4.1 K.[22] We have recently prepared a new filled skutterudite YFe_4P_{12} at high pressure.[66] The superconductivity of this compound was observed at around 7 K. Shimizu et al. have reported that iron behaves as a superconductor below 2 K at pressures between 15 and 30 GPa.[67] The superconducting transitions in $M_2Fe_3Si_5$ (M = Sc, Y and Lu) were observed at around 2–6 K.[68] YFe_4P_{12} has the highest T_c among the materials containing the ferromagnetic element Fe.

[5] Superconducting Properties of Ternary Metal Compounds. Number of valence electrons/formula unit, T_c, H_{c2} and coherence length for the superconducting materials with T_c of above 10 K are summarized in Table 6. $ZrRu_4P_2$, h-ZrRuP, h-HfRuP, ZrRuAs, ZrRhSi, h-ZrRuSi and ZrRuGe are all metal-rich compounds. On the other hand, NbPS and $LaRu_4As_{12}$ are non-metal-rich compounds. As shown in Table 1, these compounds have characteristic crystal structures. The chemical component, cell volume and number of valence electrons/formula unit for these compounds are very different. However, T_c's of the superconducting materials are between 10 and 13 K. The volume/one atom is the smallest for $ZrRu_4P_2$ (12.9 Å^3) and the largest for $LaRu_4As_{12}$ (17.3 Å^3) in these compounds. Their T_c's are not sensitive to the volume. Generally, the electrical properties of many materials depend on the number of valence electrons (including even or odd). However, the superconductivity of these materials is insensitive to the number of valence electrons. The H_{c2} value of NbPS is 17 T, higher than that of the metal-rich compounds. On the contrary, $LaRu_4As_{12}$ has a low H_{c2} value of 0.72 T. The coherence length of this arsenide is long, 206 Å. The H_{c2} values of filled skutterudite $LaRu_4X_{12}$ (X = P, As and Sb) are very small.[58]

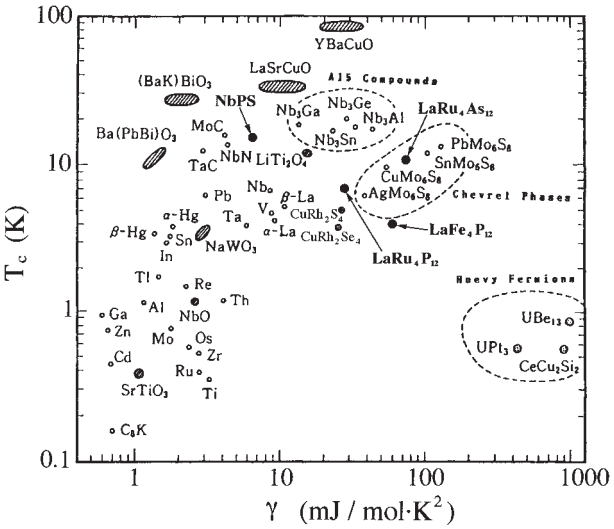

Fig. 36. Relationship between superconducting transition temperature (T_c) vs electronic specific-heat constant (γ) for various superconductors.

The electronic states at near the Fermi level for $ZrRu_4P_2$, h-ZrRuP and h-ZrRuSi with metal atom clusters in the structure are mainly due to the Ru4d character.[5,32,36] The bands of NbPS near the Fermi level are mostly of Nb d orbital character and the bands below have P and S character.[16] As shown in Table 1, the proportion of non-metal element is highest in the filled skutterudite compounds. The band calculation suggests that the electronic states of $LaRu_4P_{12}$ with P_4^{4-} clusters in the structure are due more to phosphorus rather than to the Ru4d orbital character in the vicinity of the Fermi level.[62] H_{c2} values of $ZrRu_4P_2$, h-ZrRuP and NbPS are much higher than those of $LaRu_4P_{12}$ and $LaRu_4As_{12}$. The remarkable difference of the H_{c2} value in the ternary ruthenium compounds may be closely related to the difference of the electronic states in the vicinity of the Fermi level.

Many elements, oxides, nitrides, carbides, sulfides, A15 compounds and heavy fermion compounds show the superconducting transition at various temperatures. The specific heats of these superconductors have been measured at low temperatures, and the relationship between the superconducting transition temperature (T_c) and the electronic specific-heat constant γ is discussed.[69] As mentioned above, we obtained T_c and γ for NbPS, $LaRu_4P_{12}$ and $LaRu_4As_{12}$. Figure 36 shows the relationship between T_c and γ for various superconductors. Solid circles indicate NbPS, $LaFe_4P_{12}$, $LaRu_4P_{12}$ and $LaRu_4As_{12}$. The filled skutterudites are related to the molybdenum sulfide chevrel-phase materials. NbPS is related to the niobium compounds. The specific heat of many superconducting materials prepared by us are not studied sufficiently yet. The specific heat measurement for these materials is very important in order to understand the characteristic superconducting properties.

Summary

We have prepared various ternary metal phosphides, arsenides, antimonides, silicides and germanides at high temperatures and high pressures. These superconducting materials

are classified into four groups: metal rich compounds [1] $M_2M'_4X_2$ and [2] MM′X; non-metal rich compounds MXX′ and MM'_4X_{12} (M and M′ = metal element, X and X′ = non-metal element). These compounds have the characteristic crystal structures with clusters consisting of atoms. The electrical resistivity and magnetic susceptibility of these materials were studied at low temperatures. We have found many new superconductors with T_c of above 10 K in these materials. H_{c2} values of the metal rich compounds are high, above 10 T. On the contrary, filled skutterudite $LaRu_4As_{12}$ has small H_{c2} values below 1 T. From the specific heat measurements, the electronic density of states in the vicinity of the Fermi level and Debye temperature are obtained for NbPS, $LaRu_4P_{12}$ and $LaRu_4As_{12}$. Superconducting properties of various ternary metal compounds are discussed based on the band calculations. If the electrical and magnetic properties of many materials with the similar structures and chemical components will be studied in detail, many new superconductors will be found in the near future.

The high-pressure synthesis of various compound superconductors was carried out at the Institute for Solid State Physics, the University of Tokyo. The author would like to thank Professor Takehiko Yagi, the University of Tokyo, for use of the high-pressure apparatus and for warm encouragement. Various works presented in this paper have been performed with many coworkers of Muroran Institute of Technology. The author thanks Tanaka Kikinzoku Kogyo for giving him the high-purity Ru and Os metal powders. This work was partly supported by a Grant-in-Aid for Scientific Research from the Ministry of Education, Science, Sports and Culture, No. 13874040 and No. 14204032.

References

1 G. V. S. Rao, "Advances in Solid State Chemistry," ed by C. N. R. Rao, Indian National Science Academy, New Delhi (1986), p. 292.

2 I. Shirotani, Y. Konno, D. Kato, C. Sekine, S. Todo, and T. Yagi, *Jpn. J. Appl. Phys.*, Suppl. **39-1**, 525 (2000).

3 J. M. Vandenberg and B. T. Matthias, *Science*, **198**, 194 (1977).

4 J. Y. Pivan, R. Guerin, E. H. El Ghadraoui, and M. Rafiq, *J. Less-Common Met.*, **153**, 285 (1989).

5 I. Shirotani, G. Iwasaki, I. Kaneko, C. Sekine, S. Todo, and T. Yagi, *Solid State Commun.*, **104**, 217 (1997).

6 R. Guerin and M. Sergent, *Mater. Res. Bull.*, **12**, 381 (1977).

7 S. Ishida, T. Takiguchi, S. Fujii, and S. Asano, *Physica B*, **217**, 87 (1996).

8 H. Barz, H. C. Ku, G. P. Meisner, Z. Fisk, and B. T. Mattias, *Proc. Natl. Acad. Sci. U.S.A.*, **77**, 3132 (1980).

9 R. Muller, R. N. Shelton, J. W. Richardson, and R. A. Jacobson, *J. Less-Common Met.*, **92**, 177 (1983).

10 I. Shirotani, K. Tachi, N. Ichihashi, T. Adachi, T. Kikegawa, and O. Shimomura, *Phys. Lett. A*, **205**, 77 (1995).

11 I. Shirotani, N. Ichihashi, K. Nozawa, M. Kinoshita, T. Yagi, K. Suzuki, and T. Enoki, *Jpn. J. Appl. Phys.*, Suppl. **32-3**, 695 (1993).

12 I. Shirotani, K. Tachi, K. Takeda, S. Todo, T. Yagi, and K. Kanoda, *Phys. Rev. B: Condens. Matter*, **52**, 6197 (1995).

13 I. Shirotani, M. Takaya, I. Kaneko, C. Sekine, and T. Yagi, *Solid State Commun.*, **116**, 683 (2000).

14 P. C. Donohue and P. E. Bierstedt, *Inorg. Chem.*, **8**, 2690 (1969).

15 I. Shirotani, H. Kadoya, C. Sekine, S. Todo, T. Yagi, Y. Nakazawa, and K. Kanoda, *J. Phys.: Condens. Matter*, **11**, 6231 (1999).

16 D. A. Keszler and R. Hoffmann, *J. Am. Chem. Soc.*, **109**, 118 (1987).

17 W. Jeitschko and D. Braun, *Acta Crystallogr., Sect. B*, **33**, 3401 (1977).

18 D. J. Braun and W. Jeitschko, *J. Less-Common Met.*, **72**, 147 (1980); *J. Solid State Chem.*, **32**, 357 (1980).

19 I. Shirotani, J. Hayashi, T. Adachi, C. Sekine, T. Kawakami, T. Nakanishi, H. Takahashi, J. Tang, A. Matsushita, and T. Matsumoto, *Physica B*, **322**, 408 (2002).

20 I. Shirotani, T. Uchiumi, C. Sekine, M. Hori, S. Kimura, and N. Hamaya, *J. Solid State Chem.*, **142**, 146 (1999).

21 H. Sugawara, T. D. Matsuda, K. Abe, Y. Aoki, H. Sato, S. Nojiri, Y. Inada, R. Settai, and Y. Onuki, *Phys. Rev. B: Condens. Matter*, **66**, 134411 (2002).

22 G. P. Meisner, *Physica B*, **108**, 763 (1980).

23 I. Shirotani, T. Uchiumi, K. Ohno, C. Sekine, Y. Nakazawa, and K. Kanoda, *Phys. Rev. B: Condens. Matter*, **56**, 7866 (1997).

24 C. Sekine, T. Uchiumi, I. Shirotani, and T. Yagi, *Phys. Rev. Lett.*, **79**, 3218 (1997).

25 E. D. Bauer, N. F. Frederick, P.-C. Ho, V. S. Zapf, and M. B. Maple, *Phys. Rev. B: Condens. Matter*, **65**, 100506 (2002).

26 H. Sugawara, S. Osaki, S. R. Saha, Y. Aoki, H. Sato, Y. Inada, H. Shishido, R. Settai, Y. Onuki, H. Harima, and K. Oikawa, *Phys. Rev. B: Condens. Matter*, **66**, 220504 (2002).

27 I. Shirotani, R. Maniwa, H. Sato, A. Fukizawa, N. Sato, Y. Maruyama, T. Kajiwara, H. Inokuchi, and S. Akimoto, *Nippon Kagaku Kaishi*, **1981**, 1604.

28 I. Shirotani, *Mol. Cryst. Liq. Cryst.*, **86**, 1943 (1982).

29 A. Le Beuze, M. C. Zerrouki, R. Lissillour, R. Guerin, and W. Jeitschko, *J. Alloys Compd.*, **191**, 53 (1993).

30 I. Shirotani, G. Iwasaki, I. Kaneko, S. Todo, and T. Yagi, *Rev. High Pressure Sci. Technol.*, **7**, 697 (1998).

31 M. Tinkham, "Introduction to Superconductivity," McGraw-Hill, New York (1975).

32 D. K. Seo, J. Ren, M. H. Whangbo, and E. Canadell, *Inorg. Chem.*, **36**, 6058 (1997).

33 J. Bardeen, L. N. Cooper, and J. R. Schrieffer, *Phys. Rev.*, **108**, 1175 (1957).

34 G. R. Stewart, G. P. Meisner, and H. C. Ku, "Superconductivity in d- and f-band metals," ed by W. Buckel and W. Weber, Kernforschungszentrum, Karlsruhe (1982), p. 331.

35 H. Keiber, H. Wuhl, G. P. Meisner, and G. R. Stewart, *Low Temp. Phys.*, **55**, 11 (1984).

36 I. Hase, *Phys. Rev. B: Condens. Matter*, **65**, 174507 (2002).

37 H. Salamati, F. S. Razavi, and G. Quirion, *Physica C*, **292**, 79 (1997).

38 I. Shirotani, K. Tachi, Y. Konno, S. Todo, and T. Yagi, *Philos. Mag. B*, **79**, 767 (1999).

39 I. Shirotani, D. Kato, A. Nishimoto, and T. Yagi, *J. Phys.: Condens. Matter*, **13**, 9393 (2001).

40 G. P. Meisner, H. C. Ku, and H. Barz, *Mater. Res. Bull.*, **18**, 983 (1983).

41 I. Shirotani, K. Tachi, S. Todo, and T. Yagi, "Advanced

Materials '96- New Trends in High Pressure Research," ed by M. Akaishi et al., National Institute for Research in Inorganic Materials in Japan, Tsukuba-shi (1996), p. 331.
42 V. Johnson and W. Jeitschko, *J. Solid State Chem.*, **4**, 123 (1972).
43 W. Xian-Zhong, B. Chevalier, J. Etourneau, and P. Hagenmuller, *Mater. Res. Bull.*, **20**, 517 (1985).
44 I. Shirotani, Y. Konno, Y. Okada, C. Sekine, S. Todo, and T. Yagi, *Solid State Commun.*, **108**, 967 (1998).
45 W. Jeitschko, *Metal. Trans.*, **1**, 2963 (1970).
46 I. Shirotani, M. Hori, K. Tachi, S. Todo, and T. Yagi, *J. Alloys Compd.*, **256**, L1 (1997).
47 W. Xian-Zhong, B. Chevalier, J. Etourneau, and P. Hagenmuller, *Mater. Res. Bull.*, **22**, 331 (1987).
48 P. R. Guerin and M. Sergent, *Acta Crystallogr., Sect. B*, **33**, 2820 (1977).
49 I. Shirotani, M. Takaya, I. Kaneko, C. Sekine, and T. Yagi, "Advances in Superconductivity XII," ed by Yamashita and Tanabe, Springer (2000), p. 101.
50 W. Wong-Ng, J. A. Kaduk, L. Swartendruber, and I. Shirotani, International Union of Crystallography meeting, August (2002).
51 I. Shirotani, I. Kaneko, M. Takaya, C. Sekine, and T. Yagi, *Physica B*, **281&282**, 1024 (2000).
52 I. Shirotani, M. Takaya, I. Kaneko, C. Sekine, and T. Yagi, *Physica C*, **357-360**, 329 (2001).
53 R. D. Blaugher, J. K. Hulm, and P. N. Yocom, *J. Phys. Chem. Solids*, **26**, 2037 (1965).
54 S. Wada, T. Matsumoto, S. Takata, I. Shirotani, and C. Sekine, *J. Phys. Soc. Jpn.*, **69**, 3182 (2000).
55 W. L. McMillan, *Phys. Rev.*, **167**, 331 (1968).
56 D. L. Kepert and R. E. Marshall, *J. Less-Common Met.*, **34**, 153 (1974).
57 H. Kawamura, N. Matui, I. Nakahata, M. Kobayashi, Y. Akahama, and I. Shirotani, *Solid State Commun.*, **108**, 919 (1998).
58 T. Uchiumi, I. Shirotani, C. Sekine, S. Todo, T. Yagi, Y. Nakazawa, and K. Kanoda, *J. Phys. Chem. Solids*, **60**, 689 (1999).
59 G. P. Meisner, G. R. Stewart, M. S. Torikachvili, and M. B. Maple, "LT-17," ed by U. Eckern, A. Schmid, W. Weber, and H. Wuhl, Elsevier Science Publishers B.V. (1984), p. 771.
60 H. Takahashi, A. T. Yamamoto, N. Mori, S. Adachi, H. Yamauchi, and S. Tanaka, *Physica C*, **218**, 1 (1993).
61 I. Shirotani, K. Ohno, C. Sekine, T. Yagi, T. Kawakami, T. Nakanishi, H. Takahashi, J. Tang, A. Matsushita, and T. Matsumoto, *Physica B*, **281&282**, 1021 (2000).
62 D. Jung, M. H. Whangbo, and S. Alvarez, *Inorg. Chem.*, **29**, 225 (1990).
63 I. Shirotani, T. Adachi, K. Tachi, S. Todo, K. Nozawa, T. Yagi, and M. Kinoshita, *J. Phys. Chem. Solids*, **57**, 211 (1996).
64 C. H. Lee, H. Matsuhata, A. Yamamoto, T. Ohta, H. Takazawa, K. Ueno, C. Sekine, I. Shirotani, and T. Hirayama, *J. Phys.: Condens. Matter*, **13**, L45 (2001).
65 H. Sato, Y. Abe, H. Okada, T. D. Matsuda, K. Abe, H. Sugawara, and Y. Aoki, *Phys. Rev. B: Condens. Matter*, **62**, 15125 (2000).
66 I. Shirotani, Y. Shimaya, K. Kihou, C. Sekine, N. Takeda, M. Ishikawa, and T. Yagi, *J. Phys.: Condens. Matter*, in press.
67 K. Shimizu, T. Kimura, S. Furomoto, K. Takeda, K. Kotani, and K. Amaya, *Nature*, **412**, 316 (2001).
68 H. F. Braun, *Phys. Lett. A*, **75**, 386 (1980).
69 T. Hagino, Y. Sakai, N. Wada, S. Tsuji, T. Shirane, K. Kumagai, and S. Nagata, *Phys. Rev. B: Condens. Matter*, **51**, 12673 (1995).

Ichimin Shirotani was born in Tokyo, Japan. He graduated from Chiba University in 1963 with B.S degree in chemistry. He also obtained his M.S (1965) in chemistry from Tokyo University. He joined the Institute for Solid State Physics at the University of Tokyo in 1965. He obtained his Ph.D from the University of Tokyo in 1969. His research interests are in the field of the electrical and optical behavior of organic crystals at high pressures. In 1983 he moved to Muroran Institute of Technology at Muroran as an associate professor of the Department of Applied Energy Engineering. Currently, he holds a position of Professor in the Department of Electrical and Electronic Engineering, Muroran Institute of Technology. The main targets of his research are the high-pressure synthesis of new superconductors. Electrical and magnetic properties of ternary metal compounds prepared at high pressure have been studied at low temperatures. In addition, he is active in the area of the pressure-induced phase transition with synchrotron radiation.